J. Mech. Phys. Solids 169 (2022) 105068

Contents lists available at ScienceDirect

Journal of the Mechanics and Physics of Solids

journal homepage: www.elsevier.com/locate/jmps

# A novel dimensional reduction for the equilibrium study of inextensional material surfaces

Yi-Chao Chen [a,*], Roger Fosdick [b], Eliot Fried [c,*]

[a] Department of Mechanical Engineering, University of Houston, Houston, TX 77204-4006, USA
[b] Department of Aerospace Engineering and Mechanics, University of Minnesota, Minneapolis, MN 55455-0153, USA
[c] Mechanics and Materials Unit, Okinawa Institute of Science and Technology Graduate University, Okinawa, 904-0495, Japan

ARTICLE INFO

*MSC:*
74A05
74K99
74K10
49Q10
49S05
37D35
14J26
14H81

*Keywords:*
Isometric deformations
Unstretchability
Inextensibility
Bending energy
Edge tractions
Edge moments

ABSTRACT

A general framework is developed for finding the equations describing the equilibrium of an inextensional material surface with arbitrary flat reference shape that is deformed by applying tractions or moments to its edge. This is facilitated by using a representation of all isometric deformations of the material surface to convert the bending energy of the material surface to a line integral over the edge of the material surface. Euler–Lagrange equations are derived, leading to a complete and definitive set of equilibrium equations, which are a system of ordinary differential equations for the spatial directrix. Jump conditions that apply at points where the tangent and/or curvature of the edge may be discontinuous are also derived. As a simple but illustrative example, the deformation of a rectangular strip subject to various edge conditions is studied.

## 1. Introduction

Materials like everyday photocopy paper, which bend readily but are difficult to stretch or contract without tearing or creasing, are often idealized as material surfaces that can sustain only isometric deformations. The problem of modeling and, in particular, determining the equilibrium shapes of such inextensional[1] surfaces has interested researchers for more than a century, leading to a voluminous literature. Here we mention only directly relevant contributions.

There are two conventional approaches to modeling elastic material surfaces: second-grade theory and Cosserat theory. The theory of second-grade material surfaces, for which the response functions depend on the first and second surface gradients of the deformation, was developed by Cohen and DeSilva (1966, 1968) and Balaban et al. (1967), among others. Most works concern unconstrained material surfaces. To our knowledge, a variational description of inextensional material surfaces was only recently presented by Chen et al. (2018a). That description is precise within the idealized framework of inextensional material surfaces. The equilibrium equations are derived without approximation, yielding a genuinely two-dimensional theory in which the

* Corresponding authors.
*E-mail addresses:* chen@uh.edu (Y.-C. Chen), fosdick@aem.umn.edu (R. Fosdick), eliot.fried@oist.jp (E. Fried).

[1] While the term 'inextensional' is used widely in the literature on plates and shells when referring to material surface shapes that can sustain only isometric deformations, alternative terms include 'inextensible' and 'unstretchable', both of which have been used to connote the inability of a 'rod'- or 'string'-like form to be stretched or drawn out in length. Thus in this work, we prefer to use the first of these three alternatives.

https://doi.org/10.1016/j.jmps.2022.105068
Received 22 April 2022; Received in revised form 26 August 2022; Accepted 13 September 2022
Available online 20 September 2022

basic unknown quantities are functions of two variables which mark the positions of material points in space, and the resulting equilibrium conditions are partial-differential equations. The resulting framework incorporates the possibility of tractions and moments distributed over portions of the edge of the material surface.

The theory of Cosserat surfaces, in which each material point is endowed with directors, was developed by Cosserat and Cosserat (1909). Further contributions were made by Ericksen and Truesdell (1958), Green et al. (1965), Naghdi (1972), and Steigmann (1999). While most works deal with general theories of Cosserat surfaces, there are some efforts to study inextensional Cosserat surfaces, most notably the work of Crochet (1971). Like the theory of second-grade material surfaces, the theory of Cosserat surfaces is two-dimensional and gives rise to partial-differential equations.

Outside the above two approaches are some models designed specifically for inextensional material surfaces of particular geometry, such as ribbons and strips. Sadowsky (1930) studied the equilibrium shape of a developable Möbius band of infinitesimal width.[2] He reduced the bending energy from a surface integral to a line integral through an approximation over the width. This dimensional reduction effectively renders the theory one-dimensional, giving rise to ordinary-differential equations. Later, Wunderlich (1962) showed that the dimensional reduction of the bending energy can be made exact for developable Möbius bands of finite width.[3] Further developments include the works of Starostin and van der Heijden (2007), Kirby and Fried (2014), Dias and Audoly (2014), and Starostin and van der Heijden (2014).

There are unresolved issues in some of these dimensionally-reduced models. In deriving equilibrium conditions for a material surface from a variational principle, it is crucial to first identify the entire class of kinematically admissible deformations of the given material surface from its reference configuration. Most existing models are based on the parametric representation of rectifying developable surfaces, with the parameters taking values in a fixed and prescribed set. However, as Chen and Fried (2016) and Chen et al. (2018b) demonstrate, the set of such rectifying developable surfaces is *not* generally identical to the set of all kinematically admissible deformations of a single given inextensional material surface.

In standard variational approaches to characterizing mechanical equilibrium, the governing equations are the Euler–Lagrange equations arising from requiring that the first variation of a properly defined energy functional be stationary. In the existing models for rectangular strips, the energy is taken to be a functional of the midline of the strip. As such, deriving the Euler–Lagrange equations requires expressing the variation of the energy functional in terms of the variation of the midline and then invoking the fundamental lemma of the calculus of variations. To our knowledge, the existing works do not follow this practice, often citing technical difficulties, and resort to other methods to derive the equilibrium equations. The validity of such methods remains to be verified.

Moreover, in the calculus of variations, boundary conditions should be treated via the energy functional: whereas essential boundary conditions are incorporated through the prescription of the class of kinematically admissible deformations, natural boundary conditions arise from varying the energy functional. The ingredients and analysis associated with boundary conditions are missing in the existing models, excepting the two-dimensional theory of Chen et al. (2018a). Often the equilibrium equations are derived independent of considerations of the work done by any loads that might be applied to the edge of the material surface, and boundary conditions are added a posteriori.

The main objective of the present work is to develop a framework that is applicable to flat reference shapes of general geometry, whereas the various models based on Wunderlich's (1962) dimensional reduction pertain only to the particular geometry of rectangular strips. Specifically, we present a general framework that, via standard variational methods, leads to the equilibrium equations for inextensional material surfaces of essentially arbitrary planar reference shape.

To accomplish this goal, we first identify the entire class of kinematically admissible isometric deformations from a planar reference configuration of arbitrary shape to a curved surface. To perform a dimensional reduction by integrating over the generators of the deformed surface, it is important to choose a directrix that intersects *all* generators for *any* kinematically admissible deformation. We accomplish this by choosing the edge of the surface as the directrix, as depicted in Fig. 1. Other choices of directrix, such as midline in the case of a rectangular strip, will inevitably fail to intersect all generators for certain kinematically admissible deformations. In contrast, under any injective deformation, the edge of a material surface is a material curve that must be preserved regardless of reference shape. Our choice therefore ensures that the class of kinematically admissible deformations is precisely *all* possible deformed shapes of the material surface of any particular reference shape. An added advantage of choosing the edge as the directrix is that it is the actual site where tractions and moments, if present, are applied. We are consequently able to naturally incorporate edge loads in the energy functional.

Specifically, we characterize the work done by such loads through line integrals over the edge of the material surface. Our general representation theorem for all kinematically admissible deformations involves four variables, namely the referential and spatial directrices and generatrices, that satisfy a set of isometric constraint conditions. Working with those conditions, we reduce the four primitive variables to a single one, namely the directrix of the deformed surface. This effectively renders the total potential energy as a functional of the edge of the deformed surface through a dimension reduction scheme. We further express the variation of the energy functional in terms of the variation of the edge of the deformed surface and, thus, derive the associated Euler–Lagrange equations. These are the desired equilibrium equations for the material surface. A prominent feature of our formulation is that the tractions and moments applied on the edge of the material surface appear directly in the equilibrium equations. We conclude our work with a study of the deformation of a rectangular strip under various edge conditions.

[2] See Hinz and Fried (2014) for an English translation of Sadowsky's (1930) paper.

[3] See Todres (2014) for an English translation of Wunderlichs' (1962) paper.

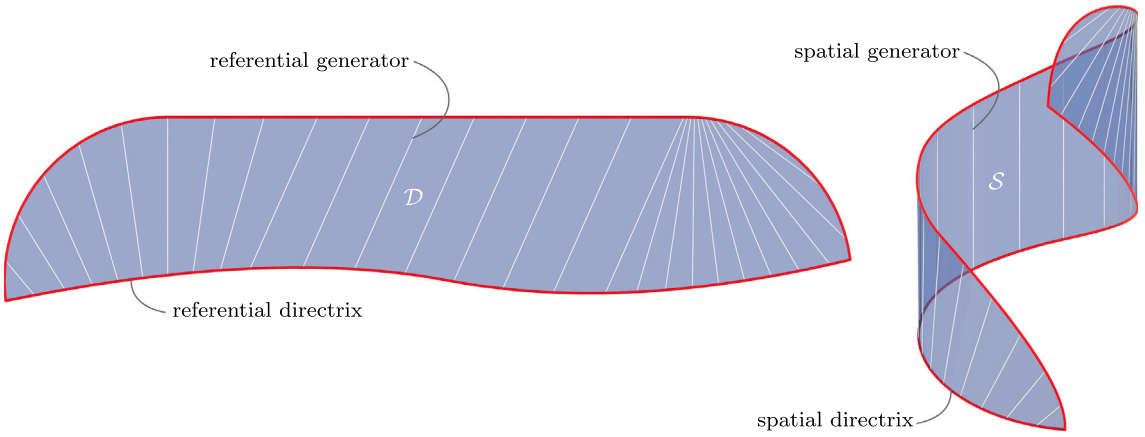


**Fig. 1.** Schematic of a planar material surface with reference configuration $\mathcal{D}$ deformed isometrically to a curved surface $\mathcal{S}$. The edges $\partial\mathcal{D}$ of $\mathcal{D}$ and $\partial\mathcal{S}$ of $\mathcal{S}$ serve as the referential and spatial directrices, respectively, and are indicated in red. Representative elements of the referential and spatial generatrices are indicated in white.

Our developments are enabled by the constraint of inextensionality, which can be viewed as the constraint of rigidity in the tangent space of the surface. It is well known that the constraint of rigidity in three dimensions leads to the representation of the entire class of rigid-body motions for a rigid body of arbitrary geometry, completely determining the kinematical framework needed to describe any such motion. This effectively reduces a three-dimensional problem to a problem for a mass point endowed with a moment of inertia, and yields algebraic equilibrium equations that are now standard fare in elementary textbooks. The classical theory of rigid-body mechanics was established in the 18th century by Euler, D'Alambert, Lagrange, and others. It is now time to devise a comprehensive counterpart of that theory for inextensional material surfaces.

## 2. Representation of deformations of inextensional material surfaces

We consider an inextensional material surface that is planar in an undistorted reference configuration $\mathcal{D}$. The material surface $\mathcal{D}$ is an open connected set in $\mathcal{E}^2$ which deforms under the action of prescribed edge forces and moments, as well as possible restrictions from prescriptions of the edge placements and tangents. A deformation of the surface is expressed by a mapping $\tilde{\boldsymbol{y}}$ from $\mathcal{D}$ to a surface $\mathcal{S}$ in three-dimensional Euclidean point space $\mathcal{E}^3$, that takes a material particle with position $\boldsymbol{x}$ in $\mathcal{D}$ to a point

$$\boldsymbol{y} = \tilde{\boldsymbol{y}}(\boldsymbol{x}) \tag{2.1}$$

belonging to $\mathcal{S}$.

We wish to find the equilibrium shape of the material surface using a variational principle which asserts that an equilibrium deformation is a stationary point of a properly defined energy functional among all kinematically admissible deformations. We first identify the set of all such deformations of $\mathcal{D}$.

An inextensional material surface can only undergo deformations in which the length of each material filament is preserved. Such deformations are called isometric. A representation for an isometric deformation has been reported by Dias and Audoly (2014, eq. (5)) and Chen et al. (2015, eqs. (24) and (47)). In those works, it is shown that if $\mathcal{D}$ isometrically deforms to a surface $\mathcal{S}$, then locally $\mathcal{D}$ and $\mathcal{S}$ must admit parametric representations of the form

$$\boldsymbol{x} = \hat{\boldsymbol{x}}(\alpha,\beta) = \boldsymbol{a}(\alpha) + \beta\boldsymbol{b}(\alpha) \qquad \text{and} \qquad \boldsymbol{y} = \hat{\boldsymbol{y}}(\alpha,\beta) = \boldsymbol{d}(\alpha) + \beta\boldsymbol{e}(\alpha), \tag{2.2}$$

where the mappings $\boldsymbol{a}$, $\boldsymbol{b}$, $\boldsymbol{d}$, and $\boldsymbol{e}$ must satisfy conditions required by the constraint of inextensionality as described below, and the common parameters $\alpha$ and $\beta$ establish a one-to-one correspondence between the material points of $\mathcal{D}$ and the material points of $\mathcal{S}$ and, hence, a deformation from $\mathcal{D}$ to $\mathcal{S}$. The representations (2.2) for $\mathcal{D}$ and $\mathcal{S}$ are those for ruled surfaces, which can be generated by the continuous motion of a straight line, called a generator (or ruling). There is a one-to-one correspondence between the generators of $\mathcal{D}$ and the generators of $\mathcal{S}$ through the parameter $\alpha$ in (2.2). Whereas Chen et al. (2015) directly used the constraint of inextensionality to derive these relations, Dias and Audoly (2014) presented them, without proof, as a corollary of the observation that an inextensional planar strip can deform only to a developable surface.

The derivation of (2.2) is based solely on local considerations and, thus, generally applies only in some neighborhood of each material point. For the purposes of the present work, we tacitly assume that the entire planar region $\mathcal{D}$ and therefore the entire surface $\mathcal{S}$ can be represented in the parametric forms (2.2), where the mappings $\boldsymbol{a}$, $\boldsymbol{b}$, $\boldsymbol{d}$, and $\boldsymbol{e}$ need not be smooth; furthermore, $\boldsymbol{b}$ and $\boldsymbol{e}$ may even be discontinuous. This permits us to consider a large class of planar reference configurations, including choices of $\mathcal{D}$ that are non-convex and connected (but possibly multiply connected), with virtually all possible arrangements of generators.

The constraint of inextensionality places restrictions on the functions $\hat{\boldsymbol{x}}$ and $\hat{\boldsymbol{y}}$ entering (2.2), and therefore, on the referential and spatial directrices $\boldsymbol{a}$ and $\boldsymbol{d}$ and the referential and spatial generatrices $\boldsymbol{b}$ and $\boldsymbol{e}$. Specifically, the deformation represented by (2.2) is isometric if and only if

$$|\hat{\boldsymbol{x}}_{,\alpha}| = |\hat{\boldsymbol{y}}_{,\alpha}|, \qquad |\hat{\boldsymbol{x}}_{,\beta}| = |\hat{\boldsymbol{y}}_{,\beta}|, \qquad \text{and} \qquad \hat{\boldsymbol{x}}_{,\alpha}\cdot\hat{\boldsymbol{x}}_{,\beta} = \hat{\boldsymbol{y}}_{,\alpha}\cdot\hat{\boldsymbol{y}}_{,\beta}, \tag{2.3}$$

where a comma followed by $\alpha$ or $\beta$ denotes the partial derivative with respect to the corresponding parameter. Equivalently, with reference to (2.2), the conditions in (2.3) are met if and only if

$$|\boldsymbol{b}| = 1, \qquad |\boldsymbol{e}| = 1, \qquad |\boldsymbol{a}'| = 1, \qquad |\boldsymbol{d}'| = 1, \qquad |\boldsymbol{b}'| = |\boldsymbol{e}'|, \qquad \boldsymbol{a}'\cdot\boldsymbol{b} = \boldsymbol{d}'\cdot\boldsymbol{e}, \qquad \text{and} \qquad \boldsymbol{a}'\cdot\boldsymbol{b}' = \boldsymbol{d}'\cdot\boldsymbol{e}', \tag{2.4}$$

where a prime is now and hereafter used to denote differentiation with respect to the parameter $\alpha$. Rather than being consequences of the constraint of inextensionality, the normalization conditions $(2.4)_{1\text{–}4}$ on $\boldsymbol{b}$, $\boldsymbol{e}$, $\boldsymbol{a}'$, and $\boldsymbol{d}'$ have been imposed for convenience without loss of generality.

We say that (2.2) is a representation of an isometric deformation from $\mathcal{D}$ to $\mathcal{S}$ in the sense that:

(i) for given choices of $\boldsymbol{a}$, $\boldsymbol{b}$, $\boldsymbol{d}$, and $\boldsymbol{e}$ satisfying (2.4), the relations in (2.2) define an isometric deformation $\tilde{\boldsymbol{y}}$ from $\mathcal{D}$ to $\mathcal{S}$;
(ii) for a given isometric deformation $\tilde{\boldsymbol{y}}$ from $\mathcal{D}$ to $\mathcal{S}$, there exist functions $\boldsymbol{a}$, $\boldsymbol{b}$, $\boldsymbol{d}$, and $\boldsymbol{e}$ satisfying (2.4), such that

$$\tilde{\boldsymbol{y}}(\boldsymbol{a}(\alpha) + \beta\boldsymbol{b}(\alpha)) = \boldsymbol{d}(\alpha) + \beta\boldsymbol{e}(\alpha) \tag{2.5}$$

for $\alpha$ and $\beta$ in some properly defined set $\mathcal{P}$.

As Chen et al. (2018b) explain, the parameter set $\mathcal{P}$ varies from problem to problem and can only be prescribed under certain decidedly peculiar and, thus, far from general circumstances. This is because the generators, along which the parameter $\alpha$ is constant, generally depend on the deformation. Consequently, the parameter set $\mathcal{P}$ is also dependent on the deformation and cannot generally be prescribed a priori. In general, finding an isometric deformation from an inextensional material surface with a given undistorted reference configuration $\mathcal{D}$ to a deformed configuration $\mathcal{S}$ will subsequently result in the determination of a corresponding parameter set $\mathcal{P}$.

Interpreted strictly, the terms "referential directrix" and "spatial directrix" refer to the curves parametrized by $\boldsymbol{a}$ and $\boldsymbol{d}$. However, for brevity we also apply those terms to $\boldsymbol{a}$ and $\boldsymbol{d}$. Homologously, we apply the terms "referential generatrix" and "spatial generatrix" to $\boldsymbol{b}$ and $\boldsymbol{e}$, which determine the referential and spatial generators that result from varying $\beta$ on the right-hand sides of $(2.2)_1$ or $(2.2)_2$ while holding $\alpha$ fixed.

## 3. Covering of $\mathcal{D}$. Referential directrix

An issue of essential importance in the representation (2.2) is that $\mathcal{D}$ must be completely covered by the mapping $\hat{\boldsymbol{x}}$ in $(2.2)_1$. Indeed, $\mathcal{D}$ is a prescribed planar region, while $\hat{\boldsymbol{x}}$ is dependent on the deformation of $\mathcal{D}$. Yet, $\hat{\boldsymbol{x}}$ must map the set $\mathcal{P}$ of parameters $\alpha$ and $\beta$ exactly onto $\mathcal{D}$, preserving in the process the material identity of the points that comprise both $\mathcal{D}$ and $\mathcal{S}$. As a consequence of this requirement, the set $\mathcal{P}$ is generally dependent on the deformation and cannot generally be prescribed a priori, as noted above. In spite of this, $\mathcal{P}$ is taken to be a fixed set in most of the existing literature. That practice is highly restrictive and can result in $\mathcal{D}$ not being covered by a mapping $\hat{\boldsymbol{x}}$ from a fixed set $\mathcal{P}$. In addition, it can result in situations in which $\hat{\boldsymbol{x}}$ maps $\mathcal{P}$ to a planar region which includes points not contained in $\mathcal{D}$. Hence, the practice of fixing $\mathcal{P}$ a priori is generally at odds with the need to maintain the identity of the material points comprising $\mathcal{D}$ and any deformed image $\mathcal{S}$ resulting from a deformation of $\mathcal{D}$.

A closely related issue arises in connection with the choice of referential directrix $\boldsymbol{a}$. A deformation can be equivalently represented by different referential directrices. A particular choice of the directrix is often made for convenience. Indeed, in all existing works concerning rectangular reference shapes, the midline of the rectangle is chosen as the referential directrix. This, among other things, is the source of the aforementioned covering problem, as all the generators emanating from the midline do not generally cover a rectangular strip $\mathcal{D}$ and some generators do not intersect the midline at all. Moreover, since a nonrectangular reference shape need not have a distinguished midline, applying the midline-based approach is generally problematic.

To overcome these difficulties, we propose to use the edge (or boundary) $\partial\mathcal{D}$ of $\mathcal{D}$ as the referential directrix and, thus, necessarily, by (2.5), the corresponding edge (or boundary) $\partial\mathcal{S}$ of $\mathcal{S}$ as the spatial directrix. The merit of this choice is obvious: For any deformation, each referential generator must intersect the edge. Moreover, the totality of all generators emanating from the edge provides a complete and exact covering of $\mathcal{D}$. In view of these observations, the edge $\partial\mathcal{D}$ of a reference configuration $\mathcal{D}$ is intrinsic and, thus, a natural choice for the referential directrix.

An immediate observation is that the edge $\partial\mathcal{D}$ intersects each generator twice, which implies that $\mathcal{D}$ will be covered twice if $\partial\mathcal{D}$ is taken as the referential directrix. To retain clarity, we first proceed by taking, as the directrix, a part of $\partial\mathcal{D}$ that intersects each generator only once, and subsequently in Section 7 change to the entire $\partial\mathcal{D}$ with the recognization that doing so only results in a multiplicity factor of two in the total elastic bending energy functional.

We assume that the edge $\partial\mathcal{D}$ of $\mathcal{D}$ is a closed curve of length $\iota$ without points of self-contact and, thus, that it is possible to parametrize $\partial\mathcal{D}$ by

$$\boldsymbol{x} = \tilde{\boldsymbol{x}}(\alpha), \tag{3.1}$$

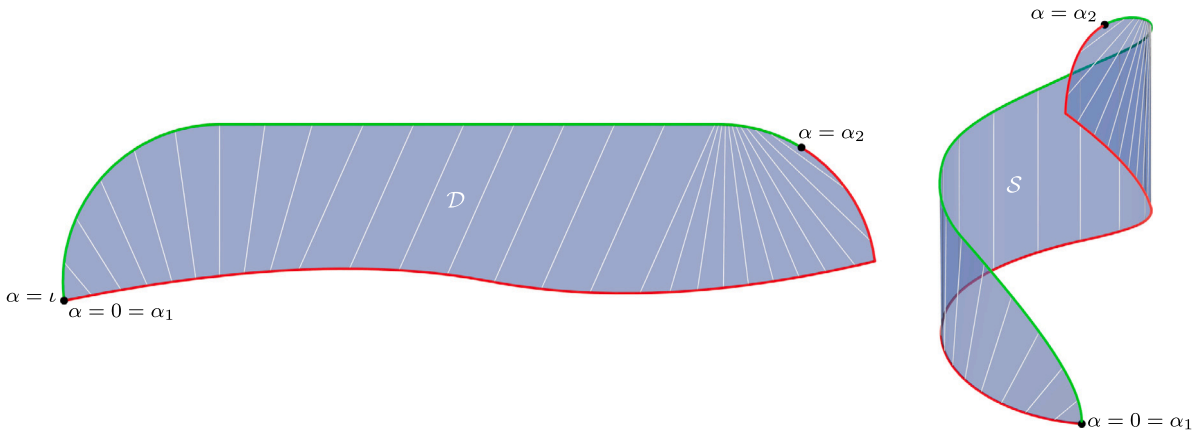


**Fig. 2.** Schematic of a planar material surface with reference configuration $\mathcal{D}$ deformed isometrically to a curved surface $\mathcal{S}$. The complete edge $\partial\mathcal{D}$ of $\mathcal{D}$ is parametrized beginning at the point labeled $\alpha = 0$ at the lower left-hand corner and ending at the same point labeled $\alpha = \iota$, the direction of traversal being counterclockwise. The subset of $\partial\mathcal{D}$ that is identified as the referential directrix begins at the point labeled $\alpha = \alpha_1 = 0$ and ends at the point labeled $\alpha = \alpha_2$. The corresponding points on the spatial directrix are also indicated. As in Fig. 1, representative elements of the referential and spatial generatrices are indicated in white.

where the mapping $\tilde{\boldsymbol{x}}$ satisfies

$$\tilde{\boldsymbol{x}}(\iota) = \tilde{\boldsymbol{x}}(0) \qquad \text{and} \qquad \tilde{\boldsymbol{x}}(\alpha_1) \neq \tilde{\boldsymbol{x}}(\alpha_2) \qquad \text{whenever} \qquad \alpha_1 \neq \alpha_2 \tag{3.2}$$

in conjunction with the normalization condition

$$|\tilde{\boldsymbol{x}}'| = 1. \tag{3.3}$$

Here, we have used $\alpha$, one of the two parameters entering the representation of the isometric deformation (2.2), as the independent variable in the parametrization (3.1) of $\partial\mathcal{D}$. This choice is consistent with the anticipated use of $\partial\mathcal{D}$ as the referential directrix.

Before using the entire edge $\partial\mathcal{D}$ of $\mathcal{D}$ as the referential directrix, we first choose an appropriate part of $\partial\mathcal{D}$ as the referential directrix. For an admissible deformation of $\mathcal{D}$ and the associated generators, there exist two points $\alpha_1$ and $\alpha_2$ on $\partial\mathcal{D}$, satisfying $0 \leq \alpha_1 < \alpha_2 < \iota$, such that all generators are sandwiched between these two points, as illustrated in Fig. 2. Without loss of generality, we take the part of $\partial\mathcal{D}$ that lies between $\alpha_1$ and $\alpha_2$ as the referential directrix:

$$\boldsymbol{a}(\alpha) \equiv \tilde{\boldsymbol{x}}(\alpha), \qquad \alpha \in [\alpha_1, \alpha_2]. \tag{3.4}$$

It is then obvious that the totality of the generators emanating from the chosen referential directrix establishes a complete and exact covering of $\mathcal{D}$. Moreover, each generator associated with $\alpha \in (\alpha_1, \alpha_2)$ intersects $\partial\mathcal{D}$ at exactly two points, $\tilde{\boldsymbol{x}}(\alpha)$ and $\tilde{\boldsymbol{x}}(\bar{\alpha})$, where $\bar{\alpha} \in (\alpha_2, \iota] \cup [0, \alpha_1)$. It therefore follows from $(2.2)_1$ that

$$\tilde{\boldsymbol{x}}(\bar{\alpha}) = \boldsymbol{a}(\alpha) + \bar{\beta}(\alpha)\boldsymbol{b}(\alpha), \tag{3.5}$$

where $\bar{\beta}(\alpha)$ is the length of the generator associated with $\alpha$. The set $\mathcal{P}$ of the parameters $\alpha$ and $\beta$ is consequently given by

$$\mathcal{P} = \{(\alpha, \beta) \in \mathbb{R}^2 : \alpha_1 \leq \alpha \leq \alpha_2, 0 \leq \beta \leq \bar{\beta}(\alpha)\}. \tag{3.6}$$

From (3.6) it is evident that $\mathcal{P}$ so defined is not a fixed set, as it depends on the deformation $\tilde{\boldsymbol{y}}$ through the associated referential generatrix $\boldsymbol{b}$.

It is required in differential geometry that the parametric representations (2.2) for $\mathcal{D}$ and $\mathcal{S}$ be regular in the sense that the vectors $\hat{\boldsymbol{x}}_{,\alpha}$ and $\hat{\boldsymbol{x}}_{,\beta}$ (and, hence, by $(2.3)_3$, the vectors $\hat{\boldsymbol{y}}_{,\alpha}$ and $\hat{\boldsymbol{y}}_{,\beta}$) are linearly independent:

$$\boldsymbol{a}' \times \boldsymbol{b} \neq \boldsymbol{0} \qquad (\text{and } \boldsymbol{d}' \times \boldsymbol{e} \neq \boldsymbol{0}). \tag{3.7}$$

Many developments in differential geometry, such as the normal vector to a surface, the area of a surface, the curvatures of a surface, and the fundamental forms of a surface, depend on this requirement. The regularity condition (3.7) requires that a generatrix not coincide with the directrix. However, in practice, we often need to consider cases in which a generatrix and the directrix coincide; this is necessary, for example, if the midline of a rectangular strip is taken as the directrix and the strip is bent about the midline. Throughout this work, we assign the boundary of $\mathcal{D}$ to be the referential directrix. If a part of the boundary of $\mathcal{D}$ is a connected straight line and a generatrix coincides with that part of $\partial\mathcal{D}$, then special considerations become necessary. In Section 9.3, we consider such a degenerate case and present a strategy for handling it.

## 4. Reduction of the kinematical variables and constraints

In variational principles of classical mechanics, an equilibrated deformation renders a properly defined energy functional stationary. For the problem at hand, a deformation of a material surface with reference configuration $\mathcal{D}$ is represented by (2.2) with the kinematical variables $\boldsymbol{a}$, $\boldsymbol{b}$, $\boldsymbol{d}$, and $\boldsymbol{e}$, which are subjected to the constraints (2.4). This leads to a constrained variational problem. A standard approach to such problems is to augment the energy functional with terms involving the constraints and associated Lagrange multiplier fields that represent reactions to the constraints. In this work, we seek to reduce the number of the constraints and, thus, Lagrange multipliers. Specifically, we will show that for the given referential directrix $\boldsymbol{a}$ and a spatial directrix $\boldsymbol{d}$ that satisfy certain reasonable conditions, the constraints (2.4) can be used to determine the referential generatrix $\boldsymbol{b}$ and the spatial generatrix $\boldsymbol{e}$. This effectively reduces the number of the kinematical variables to one, namely $\boldsymbol{d}$. A profound implication of this finding is that a prescription of an appropriate part of the edge $\partial\mathcal{S}$ determines the entire surface $\mathcal{S}$.

We establish this result in several propositions.

**Proposition 1.** *Let the referential directrix $\boldsymbol{a} : [\alpha_1, \alpha_2] \to \mathcal{E}^2$ be given by (3.4), and let a spatial directrix be given by a mapping $\boldsymbol{d} : [\alpha_1, \alpha_2] \to \mathcal{E}^3$, that satisfies $(2.4)_4$. If $\boldsymbol{d}'' \neq \boldsymbol{0}$ in $[\alpha_1, \alpha_2]$, then there exist mappings $\boldsymbol{b} : [\alpha_1, \alpha_2] \to \mathcal{V}^2$ and $\boldsymbol{e} : [\alpha_1, \alpha_2] \to \mathcal{V}^3$, as depicted in Fig. 3, that satisfy $(2.4)_{1-2,5-7}$, given respectively by*

$$\boldsymbol{b} = \cos\theta\, \boldsymbol{a}' + \sin\theta\, \boldsymbol{\jmath} \tag{4.1}$$

*and*

$$\boldsymbol{e} = \cos\theta\, \boldsymbol{d}' + \sin\theta\Big(\cos\phi\frac{\boldsymbol{d}''}{|\boldsymbol{d}''|} + \sin\phi\frac{\boldsymbol{d}'\times\boldsymbol{d}''}{|\boldsymbol{d}''|}\Big), \tag{4.2}$$

*where $\boldsymbol{\jmath}$ is a unit vector orthogonal to $\boldsymbol{a}'$ and is directed toward the interior of $\mathcal{D}$, and where the mappings $\theta : [\alpha_1, \alpha_2] \to [0, \pi]$ and $\phi : [\alpha_1, \alpha_2] \to [0, \pi]$ are given by*

$$\theta = \arctan\frac{|\boldsymbol{d}''|\sin\phi}{\tau + \phi'} \tag{4.3}$$

*and*

$$\phi = \arccos\frac{\boldsymbol{a}''\cdot\boldsymbol{\jmath}}{|\boldsymbol{d}''|}, \tag{4.4}$$

*with $\tau$, the torsion of the spatial directrix, being given by*

$$\tau = \frac{(\boldsymbol{d}'\times\boldsymbol{d}'')\cdot\boldsymbol{d}'''}{|\boldsymbol{d}''|^2}. \tag{4.5}$$

**Proof.** The condition $(2.4)_1$ follows from $(2.4)_3$ and the definition of $\boldsymbol{\jmath}$. The condition $(2.4)_2$ follows from (4.2) with the observation that $\boldsymbol{d}'$, $\boldsymbol{d}''/|\boldsymbol{d}''|$, and $\boldsymbol{d}'\times\boldsymbol{d}''/|\boldsymbol{d}''|$ are orthonormal. The condition $(2.4)_6$ follows from (4.1) and (4.2), again with the observation that $\boldsymbol{a}'$ and $\boldsymbol{\jmath}$ are orthonormal, and that $\boldsymbol{d}'$, $\boldsymbol{d}''/|\boldsymbol{d}''|$, and $\boldsymbol{d}'\times\boldsymbol{d}''/|\boldsymbol{d}''|$ are orthonormal.

Furthermore, differentiation of (4.1) and (4.2) with repeated use of the conditions $(2.4)_{1,2}$ gives

$$\boldsymbol{b}' = -\theta'\sin\theta\,\boldsymbol{a}' + \cos\theta\,\boldsymbol{a}'' + \theta'\cos\theta\,\boldsymbol{\jmath} + \sin\theta\,\boldsymbol{\jmath}' \tag{4.6}$$

and

$$\boldsymbol{e}' = -(\theta' + |\boldsymbol{d}''|\cos\phi)\sin\theta\,\boldsymbol{d}' + \Big(\cos\theta + \frac{\theta'\cos\phi\cos\theta - (\tau+\phi')\sin\phi\sin\theta}{|\boldsymbol{d}''|}\Big)\boldsymbol{d}'' + \frac{\theta'\sin\phi\cos\theta + (\tau+\phi')\cos\phi\sin\theta}{|\boldsymbol{d}''|}\boldsymbol{d}'\times\boldsymbol{d}''. \tag{4.7}$$

By (4.4), (4.6), (4.7), and the orthogonality of the various vectorial quantities, we see that

$$\boldsymbol{a}'\cdot\boldsymbol{b}' = -(\theta' + \boldsymbol{a}''\cdot\boldsymbol{\jmath})\sin\theta = -(\theta' + |\boldsymbol{d}''|\cos\phi)\sin\theta = \boldsymbol{d}'\cdot\boldsymbol{e}', \tag{4.8}$$

from which the condition $(2.4)_7$ follows. Finally, by (4.3), (4.4), (4.6), (4.7), and the orthogonality of various vector functions, we find that

$$\begin{aligned}|\boldsymbol{b}'|^2 &= (\theta' + |\boldsymbol{d}''|\cos\phi)^2\sin^2\theta + (\theta' + |\boldsymbol{d}''|\cos\phi)^2\cos^2\theta\\ &= (\theta' + |\boldsymbol{d}''|\cos\phi)^2\sin^2\theta + (|\boldsymbol{d}''|\cos\theta + \theta'\cos\phi\cos\theta - (\tau+\phi')\sin\phi\sin\theta)^2 + (\theta'\sin\phi\cos\theta + (\tau+\phi')\cos\phi\sin\theta)^2\\ &= |\boldsymbol{e}'|^2,\end{aligned} \tag{4.9}$$

which leads to $(2.4)_5$ and, thus, establishes the proposition. □

In a more general sense, the idea underlying Proposition 1 is that the action of deforming a material curve of a planar inextensional material surface to a space curve of nonvanishing curvature determines a unique surface to which the portion of the material surface between the two end generators is isometrically deformed. Specially, it has been presumed in Proposition 1 that the reference configuration $\mathcal{D}$ is between the two end generators. The conditions under which that assumption holds are presented later in this section.

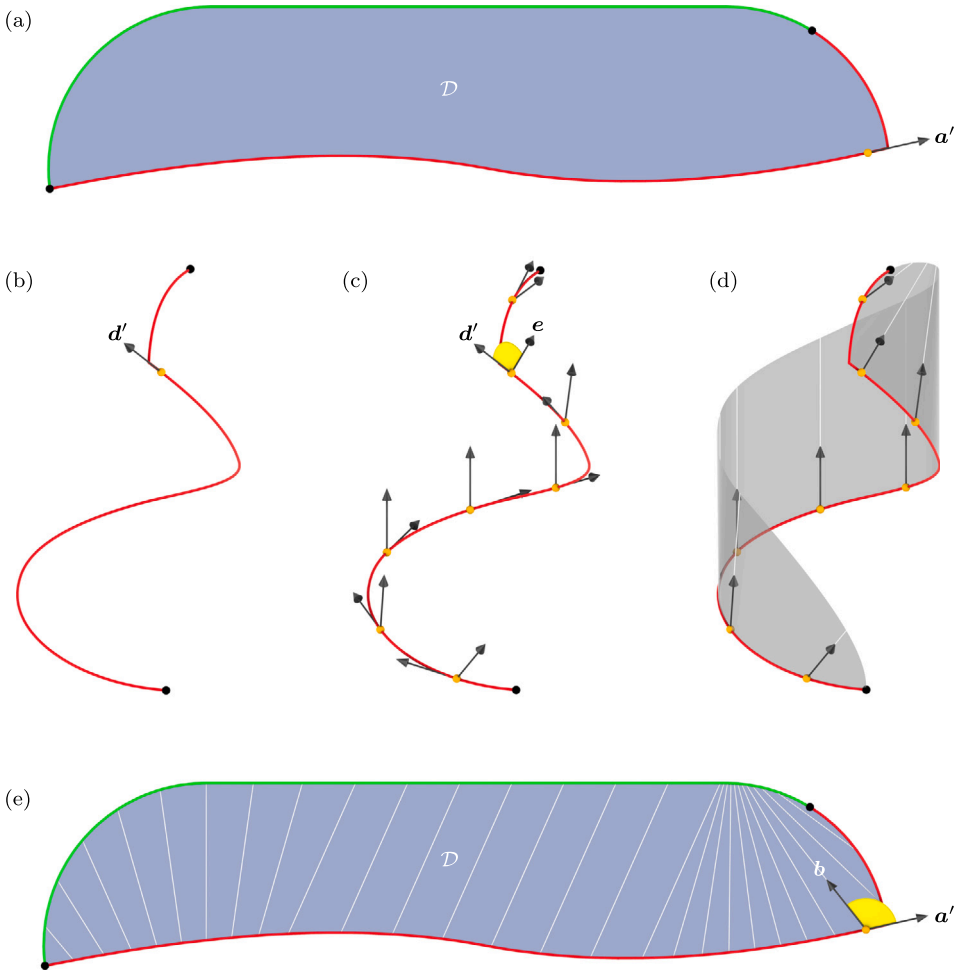


**Fig. 3.** Illustration of Proposition 1 and the generation of a developable surface from a curve: (a) The reference configuration $\mathcal{D}$, the portion of $\partial\mathcal{D}$ that serves as the anticipated referential directrix (red), and the remainder of $\partial\mathcal{D}$ (green). The unit tangent $\boldsymbol{a}'$ to the referential directrix is depicted at a representative point. (b) The assignment of a spatial directrix (red). Also depicted is the unit tangent $\boldsymbol{d}'$ at the point corresponding to the point of the reference directrix where $\boldsymbol{a}'$ appears in (a). (c) The spatial generatrix $\boldsymbol{e}$, determined by using (4.2). Also depicted is the angle $\theta$ between $\boldsymbol{d}'$ and $\boldsymbol{e}$ at the point of the spatial directrix shown in (b), determined using (4.3). (d) A portion of the developable ruled surface, indicated in gray, consisting of the continuous distribution of generators comprising the spatial generatrix. (e) Representative elements (white), of the referential generatrix, determined using (4.1). The angle $\theta$ (yellow) between $\boldsymbol{a}'$ and the corresponding referential generatrix $\boldsymbol{b}$ at the point of the referential directrix considered in (a) are also depicted. The length of each referential generator is determined consistent with (3.5).

We observe for the record that the condition

$$|\boldsymbol{d}''| \geq |\boldsymbol{a}''|, \tag{4.10}$$

which is a direct consequence of $(2.4)_{3,4,6,7}$, is imposed throughout this work. Since $(2.4)_{3,4}$ are innocuous normalization conditions and $(2.4)_{6,7}$ must hold to ensure that the deformation with parametric representation (2.2) is isometric, (4.10) is a compulsory requirement and, thus, does not constitute an additional restriction.

Proposition 1 implies that associated with a space curve $\{\boldsymbol{d}(\alpha) : \alpha_1 \leq \alpha \leq \alpha_2\}$ of nonvanishing curvature, there exists a unique developable surface, given by $(2.2)_2$, in conjunction with a planar region given by $(2.2)_1$. Next we consider the complementary case where the $\boldsymbol{d}''$ vanishes on a part of the spatial directrix $\boldsymbol{d}$.

**Proposition 2.** *Let the referential directrix $\boldsymbol{a} : [\alpha_1, \alpha_2] \to \mathcal{E}^2$ be given by (3.4), and let the spatial directrix be given by a mapping $\boldsymbol{d} : [0, \iota] \to \mathcal{E}^3$, that satisfies $(2.4)_4$. If $\boldsymbol{d}'' = \boldsymbol{0}$ in a subinterval $[\alpha_3, \alpha_4] \subset [\alpha_1, \alpha_2]$, then there exist mappings $\boldsymbol{b} : [\alpha_1, \alpha_2] \to \mathcal{V}^2$ and $\boldsymbol{e} : [\alpha_1, \alpha_2] \to \mathcal{V}^3$ that satisfy $(2.4)_{1-2,5-7}$, given respectively by*

$$\boldsymbol{b} = \cos\theta\, \boldsymbol{a}' + \sin\theta\, \boldsymbol{\jmath} \tag{4.11}$$

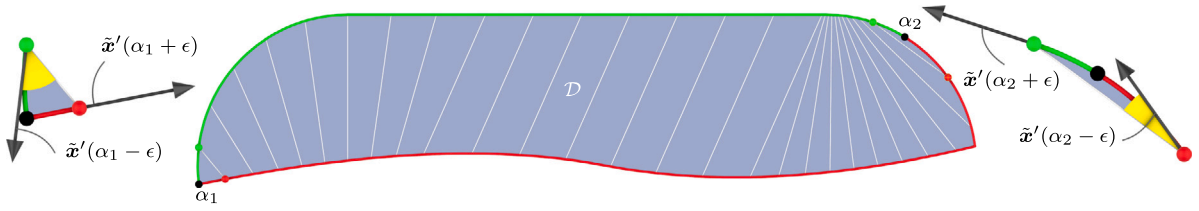


**Fig. 4.** Illustration, utilizing the planar material surface with reference configuration $\mathcal{D}$ depicted in Fig. 1, of the geometric requirement that all referential generators are between the endpoints $\tilde{\boldsymbol{x}}(\alpha_1)$ and $\tilde{\boldsymbol{x}}(\alpha_2)$ of the referential directrix. The enlarged portions of $\mathcal{D}$ are magnified by a factor of three and yellow triangles are used to represent the angles $\theta(\alpha_1-\epsilon)$ and $\theta(\alpha_2-\epsilon)$.

*and*

$$\boldsymbol{e} = \cos\theta\, \boldsymbol{d}' + \sin\theta\, \boldsymbol{g}, \tag{4.12}$$

*where* $\boldsymbol{\jmath}$ *is a unit vector orthogonal to* $\boldsymbol{a}'$ *and is directed toward the interior of* $\mathcal{D}$, $\boldsymbol{g}$ *is a constant unit vector orthogonal to* $\boldsymbol{d}'$, *and* $\theta : [\alpha_1, \alpha_2] \to [0, \pi]$ *is an arbitrary mapping.*

**Proof.** Since $|\boldsymbol{d}''| = 0$ in the subinterval $[\alpha_3, \alpha_4]$, it follows from (4.10) that $|\boldsymbol{a}''| = 0$. Hence, $\boldsymbol{a}'$, and therefore $\boldsymbol{\jmath}$, must be constant. The conditions $(2.4)_{1,2,5-7}$ follow from a similar, but much shorter, calculation to that used to establish Proposition 1. □

Unlike Proposition 1, the referential and spatial generatrices, $\boldsymbol{b}$ and $\boldsymbol{e}$, and the surface $\mathcal{S}$ generated by the spatial directrix $\boldsymbol{d}$ are not unique in Proposition 2. This is a consequence of the arbitrariness of the constant vector $\boldsymbol{g}$ and of the mapping $\theta$. If the spatial directrix $\boldsymbol{d}$ has nonvanishing curvature outside the interval $(\alpha_3, \alpha_4)$, then it is possible to choose $\boldsymbol{g}$ and $\theta$ so that the generatrices $\boldsymbol{b}$ and $\boldsymbol{e}$ and surface $\mathcal{S}$ generated from the spatial directrix $\boldsymbol{d}$ are continuous at $\alpha_3$ and $\alpha_4$.

We now wish to determine the conditions under which the planar region parametrized by $(2.2)_1$ with $\alpha \in [\alpha_1, \alpha_2]$ and $\beta \in [0, \bar{\beta}]$ is precisely $\mathcal{D}$. This requires that no two generators intersect in the interior of $\mathcal{D}$ and that the referential generators be, as discussed in the last paragraph of Section 3, sandwiched between the endpoints $\tilde{\boldsymbol{x}}(\alpha_1)$ and $\tilde{\boldsymbol{x}}(\alpha_2)$ of the referential directrix $\boldsymbol{a}$. In other words, the totality of the generators emanating from the portion of the edge $\partial\mathcal{D}$ given by $\tilde{\boldsymbol{x}}(\alpha)$, $\alpha \in [\alpha_1, \alpha_2]$, covers the given planar region $\mathcal{D}$ completely.

We note that all generators emanating from the referential directrix $\boldsymbol{d}$ cover $\mathcal{D}$ if and only if that region is between the two outermost generators passing through the endpoints $\tilde{\boldsymbol{x}}(\alpha_1)$ and $\tilde{\boldsymbol{x}}(\alpha_2)$ of the referential directrix, or, if and only if the referential generator $\beta\boldsymbol{b}(\alpha_1+\epsilon)$ and the edge near $\tilde{\boldsymbol{x}}(\alpha_1)$ form a diminishing triangle (or degenerate triangle) as $\epsilon \to 0^+$, and the referential generator $\beta\boldsymbol{b}(\alpha_2-\epsilon)$ and the edge near $\tilde{\boldsymbol{x}}(\alpha_2)$ form a diminishing triangle (or degenerate triangle) as $\epsilon \to 0^+$. A simple geometric illustration in the inserts of Fig. 4 reveals that the foregoing statements are equivalent to the conditions

$$\left.\begin{aligned} \cos\theta(\alpha_1+\epsilon) &\le -\tilde{\boldsymbol{x}}'(\alpha_1-\epsilon)\cdot\tilde{\boldsymbol{x}}'(\alpha_1+\epsilon), \qquad \text{as} \qquad \epsilon \to 0^+, \\ \cos\theta(\alpha_2-\epsilon) &\ge \tilde{\boldsymbol{x}}'(\alpha_2-\epsilon)\cdot\tilde{\boldsymbol{x}}'(\alpha_2+\epsilon), \qquad \text{as} \qquad \epsilon \to 0^+. \end{aligned}\right\} \tag{4.13}$$

The inequalities (4.13) express the requirement that the tangent lines of $\partial\mathcal{D}$ must reside on one side of the referential generators at $\tilde{\boldsymbol{x}}(\alpha_1)$ and at $\tilde{\boldsymbol{x}}(\alpha_2)$, which is equivalent to the requirement that all referential generators must reside between the point $\tilde{\boldsymbol{x}}(\alpha_1)$ and the point $\tilde{\boldsymbol{x}}(\alpha_2)$. In the case where $\partial\mathcal{D}$ is smooth at $\alpha = \alpha_1$ and $\alpha = \alpha_2$, we recognize that $\tilde{\boldsymbol{x}}'(\alpha_1-\epsilon) = \tilde{\boldsymbol{x}}'(\alpha_1+\epsilon)$ as $\epsilon \to 0^+$ and $\tilde{\boldsymbol{x}}'(\alpha_2-\epsilon) = \tilde{\boldsymbol{x}}'(\alpha_2+\epsilon)$ as $\epsilon \to 0^+$. By (4.13), $\theta$ must then satisfy

$$\theta(\alpha_1) = \pi \qquad \text{and} \qquad \theta(\alpha_2) = 0, \tag{4.14}$$

meaning that, as expected, the referential generators at the points $\boldsymbol{a}(\alpha_1)$ and $\boldsymbol{a}(\alpha_2)$ of $\partial\mathcal{D}$ are tangent to $\partial\mathcal{D}$ at those points.

We next show that no two referential generators intersect in the interior of $\mathcal{D}$ only if the condition

$$\theta' + \boldsymbol{a}''\cdot\boldsymbol{\jmath} \le \frac{\sin\theta}{\bar{\beta}(\alpha)} \tag{4.15}$$

is satisfied in the interval $(\alpha_1, \alpha_2)$. Let $\alpha$ and $\tilde{\alpha}$ be in $[\alpha_1, \alpha_2]$, with $\alpha \neq \tilde{\alpha}$. Then the generators associated with $\alpha$ and $\tilde{\alpha}$ are given, respectively, by $\boldsymbol{a}(\alpha)+\beta\boldsymbol{b}(\alpha)$ and $\boldsymbol{a}(\tilde{\alpha})+\gamma\boldsymbol{b}(\tilde{\alpha})$, with the variables $\beta$ and $\gamma$ taking values in appropriate intervals. These two generators intersect at the point

$$\boldsymbol{a}(\alpha) + \beta\boldsymbol{b}(\alpha) = \boldsymbol{a}(\tilde{\alpha}) + \gamma\boldsymbol{b}(\tilde{\alpha}). \tag{4.16}$$

Taking the scalar product of (4.16) with $\boldsymbol{b}'(\tilde{\alpha})$, we see that

$$\beta\boldsymbol{b}(\alpha)\cdot\boldsymbol{b}'(\tilde{\alpha}) = (\boldsymbol{a}(\tilde{\alpha}) - \boldsymbol{a}(\alpha))\cdot\boldsymbol{b}'(\tilde{\alpha}). \tag{4.17}$$

The assumption that two generators not intersect in the interior to $\mathcal{D}$ then requires that the condition

$$\frac{1}{\beta} = \frac{\boldsymbol{b}(\alpha)\cdot\boldsymbol{b}'(\tilde{\alpha})}{(\boldsymbol{a}(\tilde{\alpha}) - \boldsymbol{a}(\alpha))\cdot\boldsymbol{b}'(\tilde{\alpha})} \le \frac{1}{\bar{\beta}(\alpha)} \tag{4.18}$$

must hold for all $\alpha$ and $\tilde{\alpha}$, $\alpha \neq \tilde{\alpha}$, in $[\alpha_1, \alpha_2]$. Passing to the limit $\tilde{\alpha} \to \alpha$ in (4.18), we find that

$$\frac{1}{\bar{\beta}(\alpha)} \geq \lim_{\tilde{\alpha}\to\alpha} \frac{\boldsymbol{b}(\alpha)\cdot\boldsymbol{b}'(\tilde{\alpha})}{(\boldsymbol{a}(\tilde{\alpha})-\boldsymbol{a}(\alpha))\cdot\boldsymbol{b}'(\tilde{\alpha})} = -\lim_{\tilde{\alpha}\to\alpha} \frac{\boldsymbol{b}'(\alpha)\cdot\boldsymbol{b}'(\tilde{\alpha})}{\boldsymbol{a}'(\alpha)\cdot\boldsymbol{b}'(\tilde{\alpha})} = -\frac{|\boldsymbol{b}'(\alpha)|^2}{\boldsymbol{a}'(\alpha)\cdot\boldsymbol{b}'(\alpha)}, \tag{4.19}$$

which, with aid of (4.6), establishes (4.15) as a condition necessary to ensure that no two generators intersect in the interior of $\mathcal{D}$.

The above propositions establish a one-to-one correspondence between a surface $\mathcal{S}$ that is isometrically deformed from a given planar inextensional material surface with reference configuration $\mathcal{D}$ and a part of the edge $\partial\mathcal{S}$ of $\mathcal{S}$. While it is obvious that the description of $\mathcal{S}$ determines the entirety, and therefore any part of its edge $\partial\mathcal{S}$, the converse is far less apparent. That the surface $\mathcal{S}$ is completely determined by the shape of that portion of its edge $\partial\mathcal{S}$ corresponding to the spatial directrix $\boldsymbol{d}$ is a consequence of the constraint of inextensionality, as manifested by the conditions in (2.3) or the equivalent conditions in (2.4). In this regard, it is important to recognize that the endpoints $\alpha_1$ and $\alpha_2$ depend on the deformation of $\mathcal{D}$ and must be determined as part of the solution to any given problem.

It is also important to note that the construction described above is purely kinematical. As such, there is no reason to expect that any particular surface $\mathcal{S}$ generated from a part of its edge $\mathcal{S}$ by the described procedure is in a state of equilibrium. The next objective of this work is to derive the equilibrium equations and, therefore, the conditions under which the deformed surface $\mathcal{S}$ is in a state of equilibrium. As shall be seen, a remarkable finding is that any surface $\mathcal{S}$ generated as described can be maintained in equilibrium, provided the edge traction and edge moment can be assigned on $\partial\mathcal{D}$ as required. Of course, the required edge traction and edge moment satisfy certain global equilibrium conditions, that is, the resultant edge traction (including any reaction edge traction if the placement of a part of the edge is prescribed) and the resultant edge moment (including any reaction edge moment) must both vanish. This result exposes a major difference between inextensional and unconstrained material surfaces. While prescribing the placement of a part of the edge of an unconstrained material surface is not generally sufficient to determine a unique deformation of that surface, such a prescription can completely determine the deformation of an inextensional material surface. Also, an unconstrained material surface cannot generally be maintained in a deformed state of equilibrium by edge tractions and edge moments alone.

## 5. Frenet frame and Darboux frame

Reducing the active kinematical variables to the spatial directrix $\boldsymbol{d}$ enables us to express other quantities in terms of $\boldsymbol{d}$. Thus far, we have assumed that $\boldsymbol{d}$ corresponds to a portion of the edge $\partial\mathcal{S}$ of $\mathcal{S}$. For further analysis, we introduce two conventional triads, or moving frames, along the spatial directrix $\boldsymbol{d}$.

A commonly used frame associated with a space curve with parametrization $\boldsymbol{d}$ is the positively oriented Frenet triad, denoted here by $\{\boldsymbol{t}, \boldsymbol{u}, \boldsymbol{v}\}$ and defined in accord with[4]

$$\boldsymbol{t} \equiv \boldsymbol{d}', \qquad \boldsymbol{u} \equiv \frac{\boldsymbol{d}''}{|\boldsymbol{d}''|}, \qquad \text{and} \qquad \boldsymbol{v} \equiv \frac{\boldsymbol{d}'\times\boldsymbol{d}''}{|\boldsymbol{d}''|}. \tag{5.1}$$

A straightforward calculation leads to the Frenet–Serret relations

$$\boldsymbol{t}' = \kappa\boldsymbol{u}, \qquad \boldsymbol{u}' = -\kappa\boldsymbol{t} + \tau\boldsymbol{v}, \qquad \boldsymbol{v}' = -\tau\boldsymbol{u}, \tag{5.2}$$

where $\kappa$ is the curvature of $\boldsymbol{d}$, as given by

$$\kappa = |\boldsymbol{d}''|, \tag{5.3}$$

and $\tau$ is the torsion of $\boldsymbol{d}$, as given by (4.5). If $\boldsymbol{d}'' = \boldsymbol{0}$, the Frenet frame is not uniquely defined. In that case, we can identify $\boldsymbol{u}$ with any unit vector orthogonal to $\boldsymbol{d}'$ and take $\boldsymbol{v}$ to be given by $\boldsymbol{v} = \boldsymbol{t}\times\boldsymbol{u}$. Then, the Frenet–Serret relations (5.2) again hold with $\kappa = 0$ and $\tau = \boldsymbol{u}'\cdot\boldsymbol{v}$.

Since the spatial directrix $\boldsymbol{d}$ is a part of the boundary $\partial\mathcal{S}$ of the deformed surface $\mathcal{S}$, there are certain advantages to adopting the positively oriented Darboux triad $\{\boldsymbol{t}, \boldsymbol{g}, \boldsymbol{n}\}$ associated with the boundary $\partial\mathcal{S}$ of the deformed surface $\mathcal{S}$. Here, $\boldsymbol{t}$ is again the unit tangent vector along $\boldsymbol{d}$, $\boldsymbol{n}$ is a unit normal vector to $\mathcal{S}$ at the boundary $\partial\mathcal{S}$ given by

$$\boldsymbol{n} = \frac{\boldsymbol{t}\times\boldsymbol{e}}{|\boldsymbol{t}\times\boldsymbol{e}|}, \tag{5.4}$$

and $\boldsymbol{g}$ is a unit tangent-normal vector to $\partial\mathcal{S}$, given by

$$\boldsymbol{g} = \boldsymbol{n}\times\boldsymbol{t}. \tag{5.5}$$

Since $\boldsymbol{t}$ and $\boldsymbol{g}$ span the tangent space of the deformed surface $\mathcal{S}$ at its edge $\partial\mathcal{S}$, the spatial generatrix $\boldsymbol{e}$ can be conveniently expressed in terms of those vectors. Indeed, it follows from (4.2) that $\boldsymbol{t}\cdot\boldsymbol{e} = \cos\theta$, and it follows from (5.4) and (5.5) that

$$\boldsymbol{e} = (\boldsymbol{t}\cdot\boldsymbol{e})\boldsymbol{t} + |\boldsymbol{t}\times\boldsymbol{e}|\boldsymbol{g} = \cos\theta\,\boldsymbol{t} + \sin\theta\,\boldsymbol{g}. \tag{5.6}$$

[4] The unconventional symbols $\boldsymbol{u}$ and $\boldsymbol{v}$ chosen for the unit normal and unit binormal along the curve parametrized by $\boldsymbol{d}$ have been chosen to avoid conflict with the earlier use of $\boldsymbol{b}$ to denote the referential generatrix and the subsequent use of $\boldsymbol{n}$ to denote a unit normal to $\mathcal{S}$.

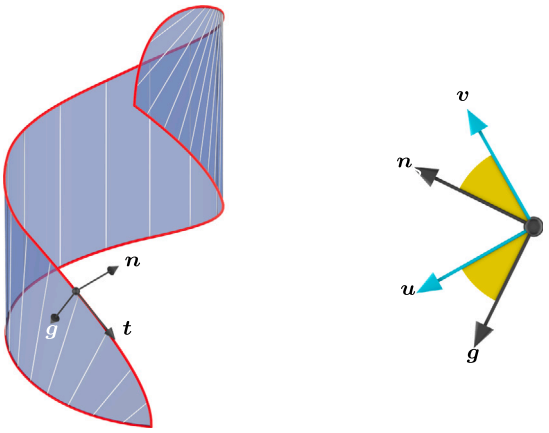


**Fig. 5.** Left: The Darboux triad $\{t, g, n\}$ at a representative point on the boundary $\partial S$ of $S$. Right: The unit normal $n$ and unit tangent-normal $g$ (black) of the Darboux frame, unit normal $u$ and unit binormal $v$ (cyan) of the Frenet frame, and angle $2\pi - \phi$ (green) at the point of the directrix shown on the left, viewed in the direction of increasing arclength along $\partial S$ (so that $t$ is directed into the page).

With reference to (4.2), (5.1), (5.4), and (5.6), we find that the base vectors of the Darboux and Frenet triads $\{t, g, n\}$ and $\{t, u, v\}$ are related by

$$g = \cos\phi\, u + \sin\phi\, v \qquad \text{and} \qquad n = -\sin\phi\, u + \cos\phi\, v, \tag{5.7}$$

where $\phi$, introduced in (4.4), defines the angle about $t$ between the two frames $\{g, n\}$ and $\{u, v\}$. By (5.2) and (5.7), we find, furthermore, that the arclength derivatives of $t$, $g$, and $n$ can be expressed as

$$t' = \kappa(\cos\phi\, g - \sin\phi\, n), \qquad g' = -\kappa\cos\phi\, t + (\tau + \phi')n, \qquad \text{and} \qquad n' = \kappa\sin\phi\, t - (\tau + \phi')g. \tag{5.8}$$

A depiction of the Darboux frame and its relation to the Frenet frame at a point on $\partial S$ is provided in Fig. 5.

## 6. Curvatures of the deformed surface

The curvatures of the deformed surface $\mathcal{S}$ are defined via the variation of a unit vector normal to $\mathcal{S}$. By the parametrization $(2.2)_2$ of $\mathcal{S}$, vectors $\hat{\boldsymbol{y}}_{,\alpha}$ and $\hat{\boldsymbol{y}}_{,\beta}$ are tangent to $\mathcal{S}$. A vector normal to $\mathcal{S}$ at a point $\hat{\boldsymbol{y}}(\alpha, \beta)$ is accordingly given by

$$\nu = \hat{\boldsymbol{y}}_{,\alpha} \times \hat{\boldsymbol{y}}_{,\beta} = (\boldsymbol{d}' + \beta \boldsymbol{e}') \times \boldsymbol{e}. \tag{6.1}$$

Using (4.3), (4.4), (5.6), and $(5.8)_{1,2}$ in (6.1), we find that $\nu$ admits an alternative representation of the form

$$\nu = (\sin\theta - \beta(\theta' + \boldsymbol{a}'' \cdot \boldsymbol{j}))\boldsymbol{d}' \times \boldsymbol{g}. \tag{6.2}$$

Granted that the point $\hat{\boldsymbol{y}}(\alpha, \beta)$ is interior to $\mathcal{S}$, we see that $0 < \beta < \bar{\beta}(\alpha)$, and, thus, by (4.15), that

$$\sin\theta - \beta(\theta' + \boldsymbol{a}'' \cdot \boldsymbol{j}) > 0. \tag{6.3}$$

A unit vector normal to $\mathcal{S}$ can then be defined by dividing $\nu$ by its magnitude, yielding

$$\frac{\nu}{|\nu|} = \boldsymbol{d}' \times \boldsymbol{g}. \tag{6.4}$$

Since both $\boldsymbol{d}$ and $\boldsymbol{g}$ depend only on $\alpha$, so does the unit normal vector defined in (6.4). Thus, the unit normal vector to $\mathcal{S}$ does not vary along a generator. Moreover, it follows from $(5.1)_1$, (5.5), and (6.4) that

$$\frac{\nu}{|\nu|} = \boldsymbol{t} \times \boldsymbol{g} = \boldsymbol{n}. \tag{6.5}$$

Hence, the unit vector normal to $\mathcal{S}$ agrees with one of the Darboux vector $\boldsymbol{n}$ defined by (5.4), and that vector will henceforth be denoted by $\boldsymbol{n}$.

In differential geometry, it is well known that the minimum normal curvature $\kappa_1$ and the maximum normal curvature $\kappa_2$ of a surface $\mathcal{S}$ with parametrization $\hat{\boldsymbol{y}} : \mathcal{P} \to \mathcal{E}^3$ can be determined by solving the eigenvalue problem

$$(II - \kappa_i I)\boldsymbol{e}_i = \boldsymbol{0}, \qquad i = 1, 2 \ \text{(no sum)}, \tag{6.6}$$

where $I$ and $II$, the matrix representations of the first and second fundamental forms of $\mathcal{S}$, are given by

$$I = \begin{bmatrix} |\hat{\boldsymbol{y}}_{,\alpha}|^2 & \hat{\boldsymbol{y}}_{,\alpha} \cdot \hat{\boldsymbol{y}}_{,\beta} \\ \hat{\boldsymbol{y}}_{,\alpha} \cdot \hat{\boldsymbol{y}}_{,\beta} & |\hat{\boldsymbol{y}}_{,\beta}|^2 \end{bmatrix} \qquad \text{and} \qquad II = \begin{bmatrix} -\hat{\boldsymbol{y}}_{,\alpha} \cdot \boldsymbol{n}_{,\alpha} & -\hat{\boldsymbol{y}}_{,\alpha} \cdot \boldsymbol{n}_{,\beta} \\ -\hat{\boldsymbol{y}}_{,\beta} \cdot \boldsymbol{n}_{,\alpha} & -\hat{\boldsymbol{y}}_{,\beta} \cdot \boldsymbol{n}_{,\beta} \end{bmatrix}, \tag{6.7}$$

respectively, and $\boldsymbol{e}_i$ represents the principal direction corresponding to the principal curvature $\kappa_i$. To determine expressions for $\kappa_1$ and $\kappa_2$ of $\mathcal{S}$, we first observe from $(2.2)_2$ and $(2.4)_2$ that

$$|\hat{\boldsymbol{y}}_{,\beta}| = 1. \tag{6.8}$$

Furthermore, since $\hat{\boldsymbol{y}}_{,\alpha}$ is in the tangent space of $\mathcal{S}$, we find, by $(2.2)_2$, that

$$\hat{\boldsymbol{y}}_{,\alpha}\cdot\boldsymbol{n} = (\boldsymbol{d}' + \beta\boldsymbol{e}')\cdot\boldsymbol{n} = -\beta\boldsymbol{e}\cdot\boldsymbol{n}' = -\beta\hat{\boldsymbol{y}}_{,\beta}\cdot\boldsymbol{n}_{,\alpha} = 0. \tag{6.9}$$

Using (6.8) and (6.9), we find that (6.6) reduces to

$$\begin{bmatrix} \hat{\boldsymbol{y}}_{,\alpha}\cdot\boldsymbol{n}_{,\alpha} + \kappa_i|\hat{\boldsymbol{y}}_{,\alpha}|^2 & \kappa_i\hat{\boldsymbol{y}}_{,\alpha}\cdot\hat{\boldsymbol{y}}_{,\beta} \\ \kappa_i\hat{\boldsymbol{y}}_{,\alpha}\cdot\hat{\boldsymbol{y}}_{,\beta} & \kappa_i \end{bmatrix}\boldsymbol{e}_i = \boldsymbol{0}, \qquad i = 1,2 \text{ (no sum)}, \tag{6.10}$$

from which we find that

$$\kappa_1 = 0 \qquad \text{and} \qquad \kappa_2 = -\frac{\hat{\boldsymbol{y}}_{,\alpha}\cdot\boldsymbol{n}_{,\alpha}}{|\hat{\boldsymbol{y}}_{,\alpha}\times\hat{\boldsymbol{y}}_{,\beta}|^2} = -\frac{\hat{\boldsymbol{y}}_{,\alpha}\cdot\boldsymbol{n}'}{|\boldsymbol{\nu}|^2}. \tag{6.11}$$

From (6.10) we also deduce that the principal direction $\boldsymbol{e}_1$ corresponding to the minimum principal curvature $\kappa_1 = 0$ is the generatrix $\boldsymbol{e}$ and that the principal direction corresponding to the maximum principal curvature $\kappa_2$ is orthogonal to $\boldsymbol{e}$. Additionally, we see from (6.11) that the mean curvature $H$ of $\mathcal{S}$ is given by

$$H = \frac{\kappa_1+\kappa_2}{2} = -\frac{\hat{\boldsymbol{y}}_{,\alpha}\cdot\boldsymbol{n}'}{2|\boldsymbol{\nu}|^2} \tag{6.12}$$

and that the Gaussian curvature $K = \kappa_1\kappa_2$ vanishes.

For subsequent reference, we observe, from (6.9), that $\boldsymbol{n}$, $\boldsymbol{n}'$, and $\hat{\boldsymbol{y}}_{,\beta}$ are mutually orthogonal. Therefore, we can write

$$\hat{\boldsymbol{y}}_{,\alpha} = \frac{\hat{\boldsymbol{y}}_{,\alpha}\cdot\boldsymbol{n}'}{|\boldsymbol{n}'|^2}\boldsymbol{n}' + (\hat{\boldsymbol{y}}_{,\alpha}\cdot\hat{\boldsymbol{y}}_{,\beta})\hat{\boldsymbol{y}}_{,\beta}. \tag{6.13}$$

Taking the scalar product with $\hat{\boldsymbol{y}}_{,\alpha}$ on both sides of (6.13) and observing from (6.1) and (6.8) that $|\hat{\boldsymbol{y}}_{,\alpha}|^2|\hat{\boldsymbol{y}}_{,\beta}|^2 - (\hat{\boldsymbol{y}}_{,\alpha}\hat{\boldsymbol{y}}_{,\beta})^2 = |\hat{\boldsymbol{y}}_{,\alpha}\times\hat{\boldsymbol{y}}_{,\beta}|^2 = |\boldsymbol{\nu}|^2$, we obtain an identity which will soon prove useful:

$$\frac{(\hat{\boldsymbol{y}}_{,\alpha}\cdot\boldsymbol{n}')^2}{|\boldsymbol{\nu}|^2} = |\boldsymbol{n}'|^2. \tag{6.14}$$

## 7. Bending energy of an inextensional elastic material surface. Dimensional reduction of the energy functional

The energy stored, per unit area, in an isotropic inextensional elastic material surface $\mathcal{S}$ with flat reference configuration $\mathcal{D}$ is entirely due to bending, as measured by the mean curvature $H$ of $\mathcal{S}$. In the simplest possible case, it is assumed that the stored energy density is a quadratic function of $H$ and, thus, that the total bending energy of the deformed surface is given by

$$E_{\mathcal{S}} = 2\mu\int_{\mathcal{S}} H^2\,\mathrm{d}a, \tag{7.1}$$

where $\mu > 0$ is a material constant called the bending modulus (or the flexural rigidity). The bending energy functional $E_{\mathcal{S}}$ defined in (7.1) is a two-dimensional surface integral. We next show that the constraint of inextensionality enables a dimensional reduction by which $E_{\mathcal{S}}$ is converted to a one-dimensional line integral.

The parametrization $\hat{\boldsymbol{y}}$ in $(2.2)_2$ maps the parameter set $\mathcal{P}$ onto the deformed surface $\mathcal{S}$. By (3.6) and (6.1), we can express $E_{\mathcal{S}}$ as an integral over $\mathcal{P}$:

$$E_{\mathcal{S}} = 2\mu\int_{\mathcal{P}} H^2|\hat{\boldsymbol{y}}_{,\alpha}\times\hat{\boldsymbol{y}}_{,\beta}|\,\mathrm{d}\alpha\,\mathrm{d}\beta = 2\mu\int_{\alpha_1}^{\alpha_2}\left(\int_0^{\bar{\beta}(\alpha)} H^2|\boldsymbol{\nu}|\,\mathrm{d}\beta\right)\mathrm{d}\alpha. \tag{7.2}$$

The inner integral in (7.2) can be carried out explicitly, converting $E_{\mathcal{S}}$ into a line integral over the spatial directrix. Specifically, by (6.12) and (6.14), we find that

$$H^2|\boldsymbol{\nu}| = \frac{(\hat{\boldsymbol{r}}_{,\alpha}\cdot\boldsymbol{n}')^2}{4|\boldsymbol{\nu}|^3} = \frac{|\boldsymbol{n}'|^2}{4|\boldsymbol{\nu}|} = \frac{|\boldsymbol{n}'|^2}{4\boldsymbol{n}\cdot\boldsymbol{\nu}_{,\beta}}\frac{\partial(\log|\boldsymbol{\nu}|)}{\partial\beta}. \tag{7.3}$$

Also, by (6.1) and the fact that the unit normal $\boldsymbol{n}$ to $\mathcal{S}$ defined in (6.5) is independent of $\beta$, we find that

$$\frac{\partial}{\partial\beta}\left(\frac{|\boldsymbol{n}'|^2}{\boldsymbol{n}\cdot\boldsymbol{\nu}_{,\beta}}\right) = 0. \tag{7.4}$$

The inner integral in (7.2) can therefore be evaluated in closed form, giving

$$\int_0^{\bar{\beta}(\alpha)} H^2|\boldsymbol{\nu}|\,\mathrm{d}\beta = \frac{|\boldsymbol{n}'|^2}{4\boldsymbol{n}\cdot\boldsymbol{\nu}_{,\beta}}\int_0^{\bar{\beta}(\alpha)}\frac{\partial(\log|\boldsymbol{\nu}|)}{\partial\beta}\,\mathrm{d}\beta = \frac{|\boldsymbol{n}'|^2}{4\boldsymbol{n}\cdot\boldsymbol{\nu}_{,\beta}}\log\frac{|\boldsymbol{\nu}(\alpha,\bar{\beta}(\alpha))|}{|\boldsymbol{\nu}(\alpha,0)|}, \tag{7.5}$$

whereby (7.2) reduces to

$$E_S = \frac{\mu}{2}\int_{\alpha_1}^{\alpha_2} \frac{|\boldsymbol{n}'|^2}{\boldsymbol{n}\cdot\boldsymbol{\nu}_{,\beta}} \log\frac{|\boldsymbol{\nu}(\alpha,\bar{\beta}(\alpha))|}{|\boldsymbol{\nu}(\alpha,0)|}\,\mathrm{d}\alpha. \tag{7.6}$$

As discussed in Section 4, a surface $\mathcal{S}$ isometrically deformed from an inextensible material surface with flat reference configuration $\mathcal{D}$ can be generated by its directrix $\boldsymbol{d}$. This enables us to express the bending energy $E_S$ as a functional of $\boldsymbol{d}$. To this end, we use (4.3), (4.4), and $(5.8)_3$ to find that

$$|\boldsymbol{n}'|^2 = \frac{|\boldsymbol{d}''|^2 - |\boldsymbol{a}''|^2}{\sin^2\theta}. \tag{7.7}$$

Also, from (5.5) and (6.2), we infer that

$$\boldsymbol{n}\cdot\boldsymbol{\nu}_{,\beta} = -(\theta' + \boldsymbol{a}''\cdot\boldsymbol{\jmath}). \tag{7.8}$$

Furthermore, from (4.15) and (6.2), we find that

$$\frac{|\boldsymbol{\nu}(\alpha,\bar{\beta}(\alpha))|}{|\boldsymbol{\nu}(\alpha,0)|} = \frac{\sin\theta(\alpha) - \bar{\beta}(\alpha)(\theta'(\alpha) + \boldsymbol{a}''(\alpha)\cdot\boldsymbol{\jmath}(\alpha))}{\sin\theta(\alpha)}, \qquad \alpha\in[\alpha_1,\alpha_2]. \tag{7.9}$$

By (7.7)–(7.9), the bending energy (7.6) can be expressed as a functional of the spatial directrix $\boldsymbol{d}$:

$$E_S = \frac{\mu}{2}\int_{\alpha_1}^{\alpha_2} \frac{|\boldsymbol{d}''|^2 - |\boldsymbol{a}''|^2}{(\theta' + \boldsymbol{a}''\cdot\boldsymbol{\jmath})\sin^2\theta} \log\frac{\sin\theta}{\sin\theta - \bar{\beta}(\theta' + \boldsymbol{a}''\cdot\boldsymbol{\jmath})}\,\mathrm{d}\alpha. \tag{7.10}$$

Notice that $\boldsymbol{a}$ in (7.10) is a known function for a given planar material surface $\mathcal{D}$, that $\theta$ is related to $\boldsymbol{d}$ through (4.3)–(4.5), and that $\bar{\beta}$ is related to $\theta$ through (3.5) and (4.1). Importantly, (7.10) encompasses situations where the referential directrix $\boldsymbol{a}$ is curved and, thus, correspondingly, situations in which its deformed image, the spatial directrix $\boldsymbol{d}$, has nontrivial geodesic curvature. The dimensional reduction leading from (7.1) to (7.10) therefore achieves one of the primary goals set in the work of Dias and Audoly (2014), but with the crucial distinction that here complete coverage of the reference shape $\mathcal{D}$ is ensured,[5] as discussed in Section 3. Furthermore, in contrast to the work of Dias and Audoly (2014), our dimensional reduction is not restricted to particular reference shapes that possess midlines.

We also observe that in (7.10) the bending energy functional is a line integral on a part of $\partial\mathcal{D}$ from $\alpha_1$ to $\alpha_2$. It can just as well be represented by a line integral on the other, complementary, part of $\partial\mathcal{D}$ running from $\alpha_2$ to $\alpha_1$. Combining these two integrals gives the line integral on the entire edge $\partial\mathcal{D}$ of the reference region $\mathcal{D}$, which equals twice of $E_S$. We may therefore express the bending energy of $\mathcal{S}$ in the form

$$E_S = \frac{\mu}{4}\int_0^{l} \frac{|\boldsymbol{d}''|^2 - |\boldsymbol{a}''|^2}{(\theta' + \boldsymbol{a}''\cdot\boldsymbol{\jmath})\sin^2\theta} \log\frac{\sin\theta}{\sin\theta - \bar{\beta}(\theta' + \boldsymbol{a}''\cdot\boldsymbol{\jmath})}\,\mathrm{d}\alpha. \tag{7.11}$$

We emphasize that when a part of the edge $\partial\mathcal{D}$ is taken as the referential directrix in (7.10), the end points $\alpha_1$ and $\alpha_2$ depend on the deformation of $\mathcal{D}$ to $\mathcal{S}$ and must be determined as a part of the solution if the problem at hand is to find the deformation. On the other hand, when the entire edge $\partial\mathcal{D}$ is taken as the referential directrix in (7.11), there is no need to identify the end points $\alpha_1$ and $\alpha_2$ that are suitable for a particular deformation, which therefore accommodates all possible isometric deformations of $\mathcal{D}$.

The equivalent dimensional reductions (7.10) and (7.11) of the bending energy (7.1) broadly generalize the Wunderlich (1962) functional. As Seguin et al. (2020) demonstrate, the Wunderlich (1962) functional provides a correct dimensional reduction of (7.1) for a rectangular strip that has been isometrically deformed into a closed knotless ribbon with any number of twists and orientability (granted that the width-to-length ratio of the strip is small enough to rule out configurations with self-contact). However, in contrast to applying only to rectangular reference shapes, (7.10) and (7.11) apply to arbitrary flat reference shapes. Moreover, whereas the Wunderlich (1962) functional involves integration over the straight midline of the reference strip, which serves as its directrix, (7.10) involves integration of a portion of the generally curved edge of the reference region, which serves as its directrix, and (7.11) involves integration over the entire edge of the reference region. Additionally, (7.10) and (7.11) provides an alternative to the dimensionally reduced energy functional of Dias and Audoly (2014, 20*). In contrast to that functional, (7.10) and (7.11) display explicit dependence on the curvature $|\boldsymbol{a}''|$ of the referential directrix $\boldsymbol{a}$ and, thus, intrinsically incorporate information about the reference region $\mathcal{D}$ through the parametrization $\boldsymbol{a}$ of its boundary $\partial\mathcal{D}$. Strictly speaking, the dimensionally reduced energy functional of Dias and Audoly (2014, 20*) is germane only to the relatively small class of reference shapes which possess well-defined midlines. However, even for such shapes, the covering issue mentioned earlier and in Footnote 5 remains.

[5] The use of a midline and the referential generatrix that intersect the midline as a coordinate cover of the reference shape will be incomplete if the continuum of all generators that pass through the midline intersects only with a part of the reference configuration, as is apparently the case for the excluded triangular-like regions near the ends of the ribbon in Fig. 1(a) Dias and Audoly (2014). For such a cover to be complete, the generators that intersect with the ends of the midline must be coincident with the ends of the reference ribbon and this places a severe restriction on the deformations that are allowable for a given reference shape.

## 8. Equilibrium equation

We seek to derive the equilibrium equation by a variational method based on the principle of virtual work for a continuous body, which asserts that the body is in an equilibrium state if and only if the work $\delta W$ that the applied loads do through an infinitesimal kinematically admissible deformation (or virtual displacement) equals the internal work done within the body in response to the infinitesimal deformation. For an inextensional elastic material surface, the work done internally in response to the infinitesimal deformation is the variation $\delta E_S$ of the bending energy $E_S$ defined in (7.1). Therefore, $S$ is in equilibrium if and only if

$$\delta E_S = \delta W \tag{8.1}$$

for all infinitesimal kinematically admissible deformations.

If the loads applied to the edge of an inextensional material surface are conservative in the sense that the work they do in deforming the reference configuration $D$ to any other admissible configuration $S$ is path independent, then that work is completely characterized by a potential $V$. This being so, the total potential energy of the system can be identified as $E_S - V$, and the principle of virtual work is manifested by the requirement that the first variation of the total potential energy vanish for all admissible variations of the deformation:

$$\delta(E_S - V) = 0. \tag{8.2}$$

The condition in (8.2) is often referred to as the principle of stationary potential energy.

In the present work, the applied loads are assumed to consist of zero body force in the interior of the surface $S$, along with a dead-load edge traction $\boldsymbol{s}$ and a dead-load edge moment $\boldsymbol{m}$ on the boundary $\partial S$ of the surface. The applied edge traction $\boldsymbol{s}$ and the applied edge moment $\boldsymbol{m}$ may be zero in a part of, or the entire, edge.

The edge traction $\boldsymbol{s}$ is assumed to be a dead load in the sense that it is a function of $\boldsymbol{x} \in \partial D$ only. The value of $\boldsymbol{s}$ gives the force per unit edge length. Therefore, the virtual work $\delta W_s$ of $\boldsymbol{s}$ through an infinitesimal kinematically admissible virtual displacement $\delta \boldsymbol{d}$ is given by

$$\int_{\partial D} \boldsymbol{s} \cdot \delta \boldsymbol{d} \, \mathrm{d}\alpha. \tag{8.3}$$

Since the applied edge traction $\boldsymbol{s}$ is independent of the deformation of the surface, we can express the virtual work (8.3) as the variation of a functional of $\boldsymbol{d}$:

$$\int_{\partial D} \boldsymbol{s} \cdot \delta \boldsymbol{d} \, \mathrm{d}\alpha = \delta \int_{\partial D} \boldsymbol{s} \cdot \boldsymbol{d} \, \mathrm{d}\alpha. \tag{8.4}$$

We thus define the potential of the edge traction by

$$V_s = \int_{\partial D} \boldsymbol{s} \cdot \boldsymbol{d} \, \mathrm{d}\alpha, \tag{8.5}$$

and we obtain $\delta W_s = \delta V_s$.

In contrast to dead-load tractions, a dead-load moment $\boldsymbol{m}$ is not conservative and therefore does not admit a potential.[6] However, the work $\delta W_m$ of $\boldsymbol{m}$ through an infinitesimal kinematically admissible virtual deformation of the surface can be readily calculated in terms of the variation of the base vectors $\{\boldsymbol{t}, \boldsymbol{g}, \boldsymbol{n}\}$ of the Darboux frame on the edge $\partial S$ of $S$. To do so, we first observe that on the edge $\partial S$ the deformation gradient can be represented by the referential surface gradient

$$\mathrm{grad}_D \tilde{\boldsymbol{y}} = \boldsymbol{t} \otimes \boldsymbol{a}' + \boldsymbol{g} \otimes \boldsymbol{\jmath}, \tag{8.6}$$

so that

$$\delta(\mathrm{grad}_D \tilde{\boldsymbol{y}}) = \mathrm{grad}_D(\delta \tilde{\boldsymbol{y}}) = \delta \boldsymbol{t} \otimes \boldsymbol{a}' + \delta \boldsymbol{g} \otimes \boldsymbol{\jmath}. \tag{8.7}$$

Next, since by the chain rule $\mathrm{grad}_D(\delta \tilde{\boldsymbol{y}}) = \mathrm{grad}_S(\delta \tilde{\boldsymbol{y}}) \mathrm{grad}_D \tilde{\boldsymbol{y}}$, where $\mathrm{grad}_S(\delta \tilde{\boldsymbol{y}})$ denotes the spatial surface gradient of the variation $\delta \tilde{\boldsymbol{y}}$ of the deformation $\tilde{\boldsymbol{y}}$, together with (8.6) and (8.7), we see that

$$\mathrm{grad}_S(\delta \tilde{\boldsymbol{y}}) = \delta \boldsymbol{t} \otimes \boldsymbol{t} + \delta \boldsymbol{g} \otimes \boldsymbol{g}, \tag{8.8}$$

which possesses a unique axial vector,[7]

$$\delta \boldsymbol{\omega} \equiv (\boldsymbol{n} \cdot \delta \boldsymbol{g}) \boldsymbol{t} + (\boldsymbol{t} \cdot \delta \boldsymbol{n}) \boldsymbol{g} + (\boldsymbol{g} \cdot \delta \boldsymbol{t}) \boldsymbol{n} \tag{8.9}$$

with the property that $(\mathrm{grad}_S(\delta \tilde{\boldsymbol{y}}))\boldsymbol{z} = \delta \boldsymbol{\omega} \times \boldsymbol{z}$ for all $\boldsymbol{z}$ in the tangent space of $S$ at the edge $\partial S$. Thus, $\delta \boldsymbol{\omega} \times \{\boldsymbol{t}, \boldsymbol{g}, \boldsymbol{n}\} = \{\delta \boldsymbol{t}, \delta \boldsymbol{g}, \delta \boldsymbol{n}\}$, and we infer that $\delta \boldsymbol{\omega}$ represents the "angular variation" of the Darboux frame $\{\boldsymbol{t}, \boldsymbol{g}, \boldsymbol{n}\}$ on the edge $\partial S$ of $S$. Consequently, the work $\delta W_m$ of $\boldsymbol{m}$ through a kinematically admissible variation of the deformation of $S$ at its edge $\partial S$ is then given by

$$\delta W_m = \int_{\partial D} \boldsymbol{m} \cdot \delta \boldsymbol{\omega} \, \mathrm{d}\alpha = \int_{\partial D} \boldsymbol{m} \cdot ((\boldsymbol{n} \cdot \delta \boldsymbol{g}) \boldsymbol{t} + (\boldsymbol{t} \cdot \delta \boldsymbol{n}) \boldsymbol{g} + (\boldsymbol{g} \cdot \delta \boldsymbol{t}) \boldsymbol{n}) \, \mathrm{d}\alpha. \tag{8.10}$$

[6] It is not commonly recognized that a constant moment, which is a special case of a dead-load moment, is not conservative. Zeigler (1977, §3.4) applied the Rodrigues–Hamilton rotation theorem to establish the path dependence of a constant moment and O'Reilly (2020, §8.7) provided an alternative proof using Euler angles.

[7] In keeping with (8.8), $\mathrm{grad}_S(\delta \tilde{\boldsymbol{y}})$ is defined only as a tensor that transforms the tangent space of $S$ at its edge $\partial S$ to $\mathcal{V}^3$.

The edge moment $\boldsymbol{m}$ is assumed to be a dead load in the sense that it is a function of $\boldsymbol{x} \in \partial D$ only. This, however, does not allow us to express the virtual work $\delta W_m$ of $\boldsymbol{m}$, given by (8.10), as the variation of a functional of kinematical quantities.

The three terms in (8.10) admit unambiguous physical interpretations. It is evident that $\boldsymbol{m}\cdot\boldsymbol{t}$ represents a bending moment, per unit edge length, about the edge of the deformed surface and that $\boldsymbol{n}\cdot\delta\boldsymbol{g}$ represents an infinitesimal rotation of the deformed surface about the edge. Hence, the term $\boldsymbol{m}\cdot((\boldsymbol{n}\cdot\delta\boldsymbol{g})\boldsymbol{t})$ represents the work of the bending moment through a variation of the surface orientation. Similarly, the term $\boldsymbol{m}\cdot((\boldsymbol{t}\cdot\delta\boldsymbol{n})\boldsymbol{g})$ represents the work of a torsional moment about the tangent-normal vector $\boldsymbol{g}$ through a variation of the surface orientation, and the term $\boldsymbol{m}\cdot((\boldsymbol{g}\cdot\delta\boldsymbol{t})\boldsymbol{n})$ represents the work of a torsional moment about the normal vector $\boldsymbol{n}$ through a variation of the surface orientation.

For further analysis, we write the work $\delta W_m$, using the expression for $\delta\boldsymbol{n}$ derived in (A.12), as

$$\begin{aligned}\delta W_m &= \int_{\partial D} \boldsymbol{m}\cdot(-(\boldsymbol{g}\cdot\delta\boldsymbol{n})\boldsymbol{t} + (\boldsymbol{t}\cdot\delta\boldsymbol{n})\boldsymbol{g} + (\boldsymbol{g}\cdot\delta\boldsymbol{t})\boldsymbol{n})\,\mathrm{d}\alpha\\ &= \int_{\partial D} \boldsymbol{m}\cdot\Big(\Big(\frac{\boldsymbol{g}}{\kappa\sin\phi}\cdot\delta\boldsymbol{d}''\Big)\boldsymbol{t} - \Big(\cos\phi\,\boldsymbol{t}\times\boldsymbol{u}\cdot\delta\boldsymbol{d}' + \frac{\sin\phi\,\boldsymbol{t}}{\kappa}\cdot\delta\boldsymbol{d}'\Big)\boldsymbol{g} + (\boldsymbol{g}\cdot\delta\boldsymbol{d}')\boldsymbol{n}\Big)\,\mathrm{d}\alpha\\ &= -\int_{\partial D} (\boldsymbol{m}_1\cdot\delta\boldsymbol{d}' - \boldsymbol{m}_2\cdot\delta\boldsymbol{d}'')\,\mathrm{d}\alpha,\end{aligned} \tag{8.11}$$

where $\boldsymbol{m}_1$ and $\boldsymbol{m}_2$ are defined according to

$$\boldsymbol{m}_1 = (\cos\phi\,\boldsymbol{v}\otimes\boldsymbol{g} - \boldsymbol{g}\otimes\boldsymbol{n})\boldsymbol{m} \qquad \text{and} \qquad \boldsymbol{m}_2 = \frac{1}{\kappa}\Big(\frac{\boldsymbol{g}\otimes\boldsymbol{t}}{\sin\phi} - \sin\phi\,\boldsymbol{t}\otimes\boldsymbol{g}\Big)\boldsymbol{m}. \tag{8.12}$$

The equilibrium states of the surface can therefore be found from the variational problem

$$\delta E_S = \delta V_s + \delta W_m = \int_0^{\iota} (\boldsymbol{s}\cdot\delta\boldsymbol{d} - \boldsymbol{m}_1\cdot\delta\boldsymbol{d}' + \boldsymbol{m}_2\cdot\delta\boldsymbol{d}'')\,\mathrm{d}\alpha. \tag{8.13}$$

For (8.13), we have used the parametric representation $\boldsymbol{x} = \boldsymbol{d}(\alpha)$, $\alpha \in [0, \iota]$, of $\partial D$.

In the present work, a certain edge placement condition may be imposed. Specifically, we may require that

$$\boldsymbol{d} = \boldsymbol{d}_0 \qquad \text{on} \qquad \partial_d D, \tag{8.14}$$

where $\boldsymbol{d}_0$ is a prescribed edge placement, and $\partial_d D$ is the portion of $\partial D$ upon which $\boldsymbol{d}_0$ is prescribed.

Two remarks of great importance on the edge placements need immediate attention:

1. We place no restrictions on the choice of $\partial_d D$. It can be any part of or, even, the entirety of $\partial D$. Applying the edge tractions and prescribing the edge placement simultaneously should create no physical and mathematical misconceptions. Indeed, the variation $\delta\boldsymbol{d} = \boldsymbol{0}$ on $\partial_d D$ implies that the virtual work of the edge traction $\boldsymbol{s}$ vanishes thereon. Also, since $\boldsymbol{d}$ is the primary variable of the variational problem (8.13), no Euler–Lagrange equation results on $\partial_d D$ since $\delta\boldsymbol{d} = \boldsymbol{0}$ on that part of $\partial D$. Therefore, the equilibrium equation to be derived is effective only on $\partial D \setminus \partial_d D$. In engineering applications, applying boundary tractions and prescribing boundary placements simultaneously is also a common practice. The applied boundary tractions, whatever they might be, will induce no deformation or motion, but only create additional reaction forces on the device used to prescribe the placements. Indeed, when the placement of the edge is prescribed, the device used to prescribe that placement applies a traction, say $\boldsymbol{s}_0$, to the edge. The edge, in turn, applies a traction $-\boldsymbol{s}_0$ to the device. If an additional traction, say $\boldsymbol{s}_1$, is applied to the edge, then the reactive traction becomes $-(\boldsymbol{s}_0 + \boldsymbol{s}_1)$ because the total traction on the edge must be $\boldsymbol{s}_0$ to ensure that the edge placement be maintained as prescribed.
2. While the prescription of the boundary placement is not restricted by the application of the edge tractions, it is restricted by the constraint of inextensionality. For example, it is obvious that the placement of any non-straight part of $\partial D$, including the union of two straight lines connected by a corner, cannot be prescribed in such a way that the deformed edge becomes straight. Such a non-straight part always exists as $\partial D$ is a planar closed curve. While the preceding example provides a necessary condition for a prescription of the edge placement to satisfy the constraint of inextensionality, it is far from being sufficient. A necessary and sufficient condition, which is termed "edge placement constraint", is given by

$$\boldsymbol{d}(\alpha) + \bar{\beta}(\alpha)\boldsymbol{e}(\alpha) = \boldsymbol{d}(\bar{\alpha}(\alpha)), \qquad \alpha \in [0, \iota], \tag{8.15}$$

where $\bar{\alpha} \geq 0$ and $\bar{\alpha}(\alpha) \in [0, \iota]$ are determined by

$$\boldsymbol{a}(\alpha) + \bar{\beta}(\alpha)\boldsymbol{b}(\alpha) = \boldsymbol{a}(\bar{\alpha}(\alpha)), \qquad \alpha \in [0, \iota], \tag{8.16}$$

with $\bar{\beta}(\alpha)$ being the length of the generator associated with $\alpha$; see (3.5). The edge placement constraint (8.15) expresses the requirement that the Euclidean distance between two material points which are connected by a generator must remain the same after deformation. Since the arrangement of the generators depends on the deformation, the edge placement constraint (8.15) is a deformation dependent, global condition.

In addition to the edge placement condition, certain "surface orientation" edge conditions may be imposed. Such conditions may prescribe the tangent vector $\boldsymbol{t} = \boldsymbol{d}'$ to the edge, or prescribe the normal vector $\boldsymbol{n}$ to the surface at the edge, or prescribe the tangent-normal vector $\boldsymbol{g}$ to the edge, or prescribe two of these three vectors. Once again, the prescription of the surface orientation edge conditions can coexist with the application of the edge tractions and the edge moments. When a surface orientation edge

condition is prescribed on a part or all of the edge where an edge moment is applied, certain components of the edge moment will not be responsible to rotate the surface, but rather induce a reactive moment on the device that prescribes the surface orientation of that part of the edge. On the other hand, the prescription of the surface orientation edge condition must be compatible with the prescription of the edge placement condition if they both are prescribed on a common part of the edge. An obvious observation is that if the edge placement is prescribed, the tangent vector $\boldsymbol{t}$ along the edge is fixed and cannot be assigned independently. As a less obvious observation, if the edge placement is such that the deformed edge is not a straight-line segment, then the orientation of the surface is completely fixed and cannot be assigned independently. Indeed, by Proposition 1, when a part of the spatial directrix has nonvanishing curvature, the spatial generators emanating from the directrix are uniquely determined by (4.2), which in turn completely determines the orientation of the deformed surface. Not only does the prescription of the edge placement to a curve of nonvanishing curvature fix the surface orientation, it also fixes the surface itself.[8] In the literature of differential geometry (see, for instance, Kreyszig and Radó (1958)), this behavior is due to the "rigidity properties of developable surfaces".

The active variable in (8.13) is the spatial directrix $\boldsymbol{d}$, which is subject to the constraint $(2.4)_4$. We now form the augmented total bending energy by incorporating the constraint $(2.4)_4$ into (7.11), giving

$$E_S^* = \int_0^l (F - \lambda(|\boldsymbol{d}'| - 1))\,\mathrm{d}\alpha, \tag{8.17}$$

where $\lambda$ is a Lagrange multiplier associated with the constraint $(2.4)_4$ ensuring that the length of the spatial directrix is preserved, and $F$ is defined through

$$F(\kappa, \theta, \theta', \bar{\beta}) \equiv \frac{\mu(\kappa^2 - |\boldsymbol{a}''|^2)}{4(\theta' + \boldsymbol{a}''\cdot\boldsymbol{j})\sin^2\theta} \log \frac{\sin\theta}{\sin\theta - \bar{\beta}(\theta' + \boldsymbol{a}''\cdot\boldsymbol{j})}. \tag{8.18}$$

The variational problem (8.13) can now be expressed as

$$\delta \int_0^l (F - \lambda(|\boldsymbol{d}'| - 1))\,\mathrm{d}\alpha = \int_0^l (\boldsymbol{s}\cdot\delta\boldsymbol{d} - \boldsymbol{m}_1\cdot\delta\boldsymbol{d}' + \boldsymbol{m}_2\cdot\delta\boldsymbol{d}'')\,\mathrm{d}\alpha. \tag{8.19}$$

The integrals in (8.19) are functionals of the spatial directrix $\boldsymbol{d}$. As discussed in Section 4, the intermediate variables $\kappa$, $\theta$, $\bar{\beta}$, $\boldsymbol{e}$, $\boldsymbol{g}$, and $\boldsymbol{n}$ can all be expressed in terms of $\boldsymbol{d}$ and its derivatives. To derive the Euler–Lagrange equation associated with (8.19), it is necessary to compute the variations of these intermediate variables in terms of the variation of $\lambda$, and the variations of $\boldsymbol{d}$ and its derivatives. Of course, the variation of $\lambda$ produces the constraint $(2.4)_4$. Detailed derivations of the remaining variations appear in Appendix A.

With reference to the identities (A.1), (A.4), (A.11), and (A.12) established in Appendix A, we find that the principle of virtual work (8.19) requires that

$$\begin{aligned}
0 &= \int_0^l \Big( \frac{\partial F}{\partial \kappa}\delta\kappa + \frac{\partial F}{\partial \theta}\delta\theta + \frac{\partial F}{\partial \theta'}\delta\theta' + \frac{\partial F}{\partial \bar{\beta}}\delta\bar{\beta} - \lambda\boldsymbol{d}'\cdot\delta\boldsymbol{d}' - \boldsymbol{s}\cdot\delta\boldsymbol{d} + \boldsymbol{m}_1\cdot\delta\boldsymbol{d}' - \boldsymbol{m}_2\cdot\delta\boldsymbol{d}'' \Big)\,\mathrm{d}\alpha \\
&= \int_0^l \Big( \frac{\partial F}{\partial \kappa}\delta\kappa + \Big( \frac{\partial F}{\partial \theta} - \bar{\beta}\cot\theta(\bar{\alpha})\frac{\partial F}{\partial \bar{\beta}} - \Big( \frac{\partial F}{\partial \theta'} \Big)' \Big)\delta\theta - \lambda\boldsymbol{d}'\cdot\delta\boldsymbol{d}' - \boldsymbol{s}\cdot\delta\boldsymbol{d} + \boldsymbol{m}_1\cdot\delta\boldsymbol{d}' - \boldsymbol{m}_2\cdot\delta\boldsymbol{d}'' \Big)\,\mathrm{d}\alpha - \Big[\!\Big[ \frac{\partial F}{\partial \theta'}\delta\theta \Big]\!\Big] \\
&= \int_0^l \Big( \frac{\partial F}{\partial \kappa}\boldsymbol{u}\cdot\delta\boldsymbol{d}'' + \Big( \frac{\partial F}{\partial \theta} - \bar{\beta}\cot\theta(\bar{\alpha})\frac{\partial F}{\partial \bar{\beta}} - \Big( \frac{\partial F}{\partial \theta'} \Big)' \Big)(\boldsymbol{h}_1\cdot\delta\boldsymbol{d}' + \boldsymbol{h}_2\cdot\delta\boldsymbol{d}'' + \boldsymbol{h}_3\cdot\delta\boldsymbol{d}''') - \lambda\boldsymbol{d}'\cdot\delta\boldsymbol{d}' \Big)\,\mathrm{d}\alpha \\
&\qquad - \int_0^l (\boldsymbol{s}\cdot\delta\boldsymbol{d} - \boldsymbol{m}_1\cdot\delta\boldsymbol{d}' + \boldsymbol{m}_2\cdot\delta\boldsymbol{d}'')\,\mathrm{d}\alpha - \Big[\!\Big[ \frac{\partial F}{\partial \theta'}(\boldsymbol{h}_1\cdot\delta\boldsymbol{d}' + \boldsymbol{h}_2\cdot\delta\boldsymbol{d}'' + \boldsymbol{h}_3\cdot\delta\boldsymbol{d}''') \Big]\!\Big].
\end{aligned} \tag{8.20}$$

Integrating by parts, we find that that (8.20) can be expressed as

$$\begin{aligned}
0 = \int_0^l &\Big( -(B\boldsymbol{h}_1)' + \Big( \frac{\partial F}{\partial \kappa}\boldsymbol{u} + B\boldsymbol{h}_2 \Big)'' - (B\boldsymbol{h}_3)''' + (\lambda\boldsymbol{d}')' - \boldsymbol{s} - \boldsymbol{m}_1' - \boldsymbol{m}_2'' \Big)\cdot\delta\boldsymbol{d}\,\mathrm{d}\alpha \\
&- \Big[\!\Big[ \Big( B\boldsymbol{h}_1 - \Big( \frac{\partial F}{\partial \kappa}\boldsymbol{u} + B\boldsymbol{h}_2 \Big)' + (B\boldsymbol{h}_3)'' - \lambda\boldsymbol{d}' + \boldsymbol{m}_1 + \boldsymbol{m}_2' \Big) \Big]\!\Big]\cdot\delta\boldsymbol{d} \\
&- \Big[\!\Big[ \Big( \frac{\partial F}{\partial \kappa}\boldsymbol{u} + \frac{\partial F}{\partial \theta'}\boldsymbol{h}_1 + B\boldsymbol{h}_2 - (B\boldsymbol{h}_3)' - \boldsymbol{m}_2 \Big)\cdot\delta\boldsymbol{d}' + \Big( \frac{\partial F}{\partial \theta'}\boldsymbol{h}_2 + B\boldsymbol{h}_3 \Big)\cdot\delta\boldsymbol{d}'' + \frac{\partial F}{\partial \theta'}\boldsymbol{h}_3\cdot\delta\boldsymbol{d}''' \Big]\!\Big],
\end{aligned} \tag{8.21}$$

where $B$, $\boldsymbol{h}_1$, $\boldsymbol{h}_2$, and $\boldsymbol{h}_3$ are defined according to

$$\left.\begin{aligned}
B &= \frac{\partial F}{\partial \theta} - \Big( \frac{\partial F}{\partial \theta'} \Big)' - \bar{\beta}\cot\theta(\bar{\alpha})\frac{\partial F}{\partial \bar{\beta}}, \qquad \boldsymbol{h}_1 = -\frac{\sin^2\theta}{\kappa\sin\phi}(\tau\boldsymbol{t} + \kappa\boldsymbol{v}), \\
\boldsymbol{h}_2 &= \frac{\sin^2\theta}{\kappa\sin^2\phi}\Big( \cos\phi\,\boldsymbol{t} + 2\cot\theta\,\boldsymbol{u} + \frac{\kappa' - \kappa\tau\cot\phi}{\kappa^2}\boldsymbol{g} \Big), \qquad \text{and} \qquad \boldsymbol{h}_3 = -\frac{\sin^2\theta}{\kappa^2\sin^2\phi}\boldsymbol{g},
\end{aligned}\right\} \tag{8.22}$$

the quantity $\bar{\alpha}$ is determined, according to (8.16), by

$$\boldsymbol{a}(\bar{\alpha}) = \boldsymbol{a}(\alpha) + \bar{\beta}(\alpha)\boldsymbol{b}(\alpha), \qquad \alpha \in [0, l], \tag{8.23}$$

[8] For example, fixing one edge of an inextensional rectangular strip to a circular path drawn on a flat plane produces a right circular cylindrical surface shape.

the jump $[\![f]\!]$ of a function $f$ at some $\alpha \in [0, \imath]$ is defined by

$$[\![f(\alpha)]\!] = \lim_{\epsilon \to 0^+} (f(\alpha + \epsilon) - f(\alpha - \epsilon)), \tag{8.24}$$

and the continuity of $\delta \boldsymbol{d}$, which is a consequence of the basic requirement that $\boldsymbol{d}$ be continuous, has been used. As a reminder, the vectors $\boldsymbol{t}$, $\boldsymbol{u}$, and $\boldsymbol{v}$, $\boldsymbol{g}$, and $\boldsymbol{n}$ in (8.22) are defined through (5.1), (5.4), and (5.5).

In (8.21), we have tactically left the point where the jumps are evaluated unspecified. That jump can actually occur any point in the interval $[0, \imath]$. Indeed, we can take a number of points in the interval and include the jumps at these points in (8.21). Of course, if the quantity in a jump operator is continuous, then the jump is zero and there is no need to include the said jump term. Hence, in practice, only the points where the jump is potentially non-zero are of interest. There are various sources for such discontinuities. For example, if the referential directrix is not smooth at some point, the spatial directrix will also be non-smooth and certain jump conditions (or corner conditions as often appropriately called) must be satisfied.

Applying the fundamental theorem of calculus of variations to (8.21), we obtain the Euler–Lagrange equation for the variational problem (8.13):

$$-(B\boldsymbol{h}_1)' + \Big(\frac{\partial F}{\partial \kappa}\boldsymbol{u} + B\boldsymbol{h}_2\Big)'' - (B\boldsymbol{h}_3)''' + (\lambda \boldsymbol{d}')' = \boldsymbol{s} + \boldsymbol{m}_1' + \boldsymbol{m}_2''. \tag{8.25}$$

The equation of equilibrium (8.25) must hold on $\partial \mathcal{D} \setminus \partial_d \mathcal{D}$, where the edge placement $\boldsymbol{d}$ is not prescribed. On $\partial_d \mathcal{D}$ where the placement is prescribed, the edge placement condition (8.14) must be satisfied instead of (8.25). In the special case in which $\partial_d \mathcal{D} = \partial \mathcal{D}$, meaning that the placement of the entire edge is prescribed (subject to the edge placement constraint (8.15)), the equation of equilibrium (8.25) is void and unneeded, and the deformed surface is determined by $(2.2)_2$ and Propositions 1 and 2.

Apart from the Euler–Lagrange equation (8.25), various jump conditions can be derived from (8.21) as consequences of specifying conditions on $\delta \boldsymbol{d}'$, $\delta \boldsymbol{d}''$, and $\delta \boldsymbol{d}'''$. In particular, the jump condition

$$\Big[\!\Big[ B\boldsymbol{h}_1 - \Big(\frac{\partial F}{\partial \kappa}\boldsymbol{u} + B\boldsymbol{h}_2\Big)' + (B\boldsymbol{h}_3)'' - \lambda \boldsymbol{d}' + \boldsymbol{m}_1 + \boldsymbol{m}_2' \Big]\!\Big] = \boldsymbol{0} \tag{8.26}$$

must hold throughout $\partial \mathcal{D} \setminus \partial_d \mathcal{D}$. In view of (8.25), the jump condition (8.26) is satisfied if and only if the edge traction $\boldsymbol{s}$ is bounded. In contrast to $\delta \boldsymbol{d}$, the variations $\delta \boldsymbol{d}'$, $\delta \boldsymbol{d}''$, and $\delta \boldsymbol{d}'''$ of $\boldsymbol{d}'$, $\boldsymbol{d}''$, and $\boldsymbol{d}'''$ need not be continuous on $[0, \imath]$. However, $\delta \boldsymbol{d}'$, $\delta \boldsymbol{d}''$, and $\delta \boldsymbol{d}'''$ must be consistent with the constraints (2.4) that impose the isometry of the deformation. In particular, since (2.4) requires that the angle between any two infinitesimal material filaments be preserved under any smooth deformation of $\mathcal{D}$, $\delta \boldsymbol{d}'$ must satisfy

$$[\![\boldsymbol{t} \cdot \delta \boldsymbol{d}']\!] = 0, \qquad [\![\boldsymbol{g} \cdot \delta \boldsymbol{d}']\!] = 0, \qquad \text{and} \qquad [\![\boldsymbol{n} \cdot \delta \boldsymbol{d}']\!] = 0; \tag{8.27}$$

in other words, the components of $\delta \boldsymbol{d}'$ relative to the Darboux frame $\{\boldsymbol{t}, \boldsymbol{g}, \boldsymbol{n}\}$ must be continuous.[9] Using (8.27) and the consequence $\boldsymbol{t} \cdot \delta \boldsymbol{d}' = 0$ of varying the constraint $(2.4)_4$ in (8.21), we obtain a pair of jump conditions:

$$\left.\begin{aligned} \Big[\!\Big[ \sin\phi \frac{\partial F}{\partial \kappa} + \frac{B \sin\theta \cos\theta}{\kappa \sin\phi} \Big]\!\Big] &= 0, \\ \Big[\!\Big[ \cos\phi \frac{\partial F}{\partial \kappa} - \frac{\sin^2\theta}{\sin^2\phi}\frac{\partial F}{\partial \theta'} + \frac{B \sin\theta\cos\theta\cos\phi}{\kappa \sin^2\phi} + \frac{1}{\kappa \sin\phi}\Big(\frac{B \sin^2\theta}{\kappa \sin\phi}\Big)' - \frac{\boldsymbol{m}\cdot\boldsymbol{t}}{\kappa \sin\phi} \Big]\!\Big] &= 0. \end{aligned}\right\} \tag{8.28}$$

A derivation in Appendix B shows that (8.28) stem from a vectorial condition with no tangential component; $(8.28)_1$ and $(8.28)_2$ are the components of that condition in the directions of $\boldsymbol{g}$ and $\boldsymbol{n}$, respectively. If we also stipulate the components of $\delta \boldsymbol{d}''$ relative to $\{\boldsymbol{t}, \boldsymbol{g}, \boldsymbol{n}\}$ are continuous, then we obtain another pair of jump conditions from (8.21):

$$\left.\begin{aligned} \Big[\!\Big[ \frac{\sin\theta\cos\theta}{\kappa \sin\phi}\frac{\partial F}{\partial \theta'} \Big]\!\Big] &= 0, \\ \Big[\!\Big[ \frac{\sin^2\theta}{\kappa \sin^2\phi}\Big(\cot\theta\cos\phi + \frac{\kappa' + \kappa\phi' \cot\phi}{\kappa^2}\Big)\frac{\partial F}{\partial \theta'} - \frac{B \sin^2\theta}{\kappa^2 \sin^2\phi} \Big]\!\Big] &= 0. \end{aligned}\right\} \tag{8.29}$$

Like (8.28), $(8.29)_1$ and $(8.29)_2$ are the components in the directions of $\boldsymbol{g}$ and $\boldsymbol{n}$, respectively, of a vectorial precursor with no tangential component. Finally, if we also require that the components of $\delta \boldsymbol{d}'''$ relative to $\{\boldsymbol{t}, \boldsymbol{g}, \boldsymbol{n}\}$ are continuous, we obtain another jump condition from (8.21):

$$\Big[\!\Big[ \frac{\sin^2\theta}{\kappa^2 \sin^2\phi}\frac{\partial F}{\partial \theta'} \Big]\!\Big] = 0. \tag{8.30}$$

This final jump condition arises from a vectorial condition which involves only a component in the direction of $\boldsymbol{g}$.

The jump conditions (8.26) and (8.28)–(8.30) must be satisfied at corner points of $\partial \mathcal{D} \setminus \partial_d \mathcal{D}$, where $\boldsymbol{a}'$ and, possibly, $\boldsymbol{a}''$ or $\boldsymbol{a}'''$ are discontinuous. They also apply at points of $\partial \mathcal{D} \setminus \partial_d \mathcal{D}$ where $\boldsymbol{a}'$ is continuous but either $\boldsymbol{a}''$ or $\boldsymbol{a}'''$ is discontinuous. The quantities that appear within each of the jumps in (8.26) and (8.28)–(8.30) must also be continuous at any point of $\partial \mathcal{D} \setminus \partial_d \mathcal{D}$ where the referential directrix is smooth.

[9] The conditions in (8.27) are equivalent to the condition $[\![\delta \boldsymbol{d}']\!] = \boldsymbol{0}$ if and only if elements $\boldsymbol{t}$, $\boldsymbol{g}$, and $\boldsymbol{n}$ of the Darboux frame satisfy $[\![\boldsymbol{t}]\!] = \boldsymbol{0}$, $[\![\boldsymbol{g}]\!] = \boldsymbol{0}$, and $[\![\boldsymbol{n}]\!] = \boldsymbol{0}$. But, at a corner on a smooth surface the limiting values $\boldsymbol{n}^{\pm}$ of the normal $\boldsymbol{n}$ are equal: $\boldsymbol{n}^+ = \boldsymbol{n}^- =: \boldsymbol{n}$; moreover, the limiting values $\boldsymbol{t}^{\pm}$ and $\boldsymbol{g}^{\pm}$ of the tangent and tangent normal at the corner obey $\boldsymbol{t}^+ = \boldsymbol{R}\boldsymbol{t}^-$ and $\boldsymbol{g}^+ = \boldsymbol{R}\boldsymbol{g}^-$, where $\boldsymbol{R}$ is a rotation, about the axis $\boldsymbol{n}$, by the exterior angle of the corner.

It is noteworthy that the equation of equilibrium (8.25) can be recast, by introducing certain auxiliary variables, in a form resembling the equations of equilibrium commonly encountered in the Kirchhoff rod theory. If we introduce variables $\boldsymbol{f}$ and $\boldsymbol{h}$ through

$$\left.\begin{aligned} \boldsymbol{f} &\equiv B\boldsymbol{h}_1 - \left(\frac{\partial F}{\partial \kappa}\boldsymbol{u} + B\boldsymbol{h}_2\right)' + (B\boldsymbol{h}_3)'' - \lambda \boldsymbol{t} + \boldsymbol{m}_1 + \boldsymbol{m}_2', \\ \boldsymbol{h} &\equiv \boldsymbol{t} \times \left(\frac{\partial F}{\partial \kappa}\boldsymbol{u} + B\boldsymbol{h}_2 - (B\boldsymbol{h}_3)' - \boldsymbol{m}_2\right) + \kappa B\boldsymbol{u} \times \boldsymbol{h}_3, \end{aligned}\right\} \tag{8.31}$$

then (8.25) can be written as

$$\boldsymbol{f}' + \boldsymbol{s} = \boldsymbol{0}. \tag{8.32}$$

Furthermore, it follows from (8.22) and (8.31) that

$$\boldsymbol{h}' + \boldsymbol{t} \times \boldsymbol{f} + \boldsymbol{m} = \boldsymbol{0}. \tag{8.33}$$

The conditions (8.32) and (8.33) have the same formal structure, respectively, as the force balance and the moment balance that arise in the theory of Kirchhoff rods. On this basis, it might be tempting to identity $\boldsymbol{f}$ as a measure of internal force and $\boldsymbol{h}$ as a measure of the internal moment. We must, however, stress that recasting (8.25) in the form of (8.32) and (8.33) does not imply the existence of a kinetic analogue between the theory of inextensional material surfaces and the theory of Kirchhoff rods. Indeed, whereas the internal force and the internal moment arising in the theory of Kirchhoff rods are independent, the quantities $\boldsymbol{f}$ and $\boldsymbol{h}$ defined through (8.31) are not independent. Consequently, (8.32) and (8.33) are not independent. Indeed, while (8.31) and (8.32) are equivalent to (8.25), (8.33) is simply an identity that follows from (8.31).

The Euler–Lagrange equation (8.25) and the constraint $(2.4)_4$ are ordinary-differential equations. These equations can be solved to determine the equilibrium configuration $\mathcal{S}$ of the material surface with reference configuration $\mathcal{D}$ and subjected to the edge loads $\boldsymbol{s}$ and $\boldsymbol{m}$, along with appropriate placement and surface orientation edge conditions.

On the other hand, it can be observed that the Euler–Lagrange equation (8.25) and the constraint $(2.4)_4$ can be satisfied by appropriate choices of the edge traction $\boldsymbol{s}$ or edge moment $\boldsymbol{m}$. In Section 4, we have shown that a surface $\mathcal{S}$ that is isometrically deformed from an inextensional material surface with planar reference configuration $\mathcal{D}$ can be generated by a space curve. Now we have furthermore established that any such surface $\mathcal{S}$ can be maintained in equilibrium by suitable choices of the edge loads $\boldsymbol{s}$ and $\boldsymbol{m}$. The choices are not unique. In particular, it is always possible to choose $\boldsymbol{m} = \boldsymbol{0}$ and find $\boldsymbol{s}$ such that (8.25) is satisfied, or to choose $\boldsymbol{s} = \boldsymbol{0}$ and find $\boldsymbol{m}$ such that the same holds. Thus, a combination of an edge traction and an edge moment on a common subset of $\partial\mathcal{D} \setminus \partial_d\mathcal{D}$ can be replaced entirely by an edge traction or an edge moment. This indeterminacy arises as a consequence of the highly restrictive nature of the constraint of inextensionality and its relationship to a sort of 2D rigidity, and has been observed previously by Chen et al. (2018a) in the analysis of the semi-inverse problems involving the isometric bending of a rectangular strip onto a right-circular conical surface and onto a cylindrical surface.

## 9. An illustrative example

To demonstrate the utility of the current theory in finding the equilibrium configurations of inextensional material surfaces under edge loads, we present elementary solutions for a rectangular reference strip. As the distinguishing features of the current theory stem from its applicability to material surfaces of arbitrary reference geometry, we will present detailed solutions for non-rectangular reference configurations elsewhere.

One purpose of presenting this simple example is to illustrate the effects of various edge conditions on the equilibrium configuration of the deformed surface. To this end, we assume that the surface is subjected to no placement and orientation edge conditions and vanishing edge traction and zero edge moment on two parallel edges, and is subjected to one of the four combinations of the edge conditions on the other two parallel edges:

1. Connecting edge placements and equal orientation tangent-normal vectors;
2. Connecting edge placements and opposite orientation tangent-normal vectors;
3. Zero edge traction, and non-zero edge moment;
4. Connecting edge placements and zero edge moment.

The reference configuration $\mathcal{D}$ can be represented by

$$\mathcal{D} \equiv \{\boldsymbol{x} \in \mathcal{E}^2 : \boldsymbol{x} = x_1\boldsymbol{\imath} + x_2\boldsymbol{\jmath}, x_1 \in [0, l_1], x_2 \in [0, l_2]\}, \tag{9.1}$$

where $\boldsymbol{\imath}$ and $\boldsymbol{\jmath}$ are two orthonormal vectors, and where $l_1$ and $l_2$ are the lengths of the two perpendicular edges. We will designate Edge I, II, III, and IV as those associated, respectively, with $x_2 = 0$, $x_1 = l_1$, $x_2 = l_2$, and $x_1 = 0$. We assume that Edges I and III are subjected to neither placement nor orientation edge conditions but are subjected to zero edge traction and zero edge moment while Edges II and IV are subjected to one of the four edge conditions listed above. We also assume that Edges II and IV move without twisting the rectangular reference strip. Under these conditions, the rectangular reference configuration will deform into a cylindrical surface, for which Edges I and III will be deformed into two parallel planar curves, Edges II and IV will be deformed into two parallel straight lines perpendicular to the planes of the deformed Edges I and III, and the generators of the deformed surface

will consist of parallel straight lines perpendicular to the planes. Hence, the equilibrium configuration of the deformed surface is completely determined by the shape of the deformed Edge I.

Edge I has zero curvature in the reference configuration, and is assumed to have non-zero curvature in the deformed configuration. It then follows from (4.4) that $\phi = \pi/2$. Also, since Edge I is a planar curve after deformation, we have that $\tau = 0$, and it follows from (4.3) that $\theta = \pi/2$. By using (4.1), (4.2), (3.5), and (5.7), we find, corresponding to Edge I, that

$$\boldsymbol{b} = \boldsymbol{j}, \qquad \bar{\beta} = l_2, \qquad \boldsymbol{e} = \boldsymbol{t} \times \boldsymbol{u}, \qquad \boldsymbol{g} = \boldsymbol{v}, \qquad \boldsymbol{n} = -\boldsymbol{u}. \tag{9.2}$$

Moreover, by (8.18) and (8.22), we find that

$$\frac{\partial F}{\partial \kappa} = \frac{\mu l_2}{2}\kappa, \qquad B = -\frac{\mu l_2^2}{4}\kappa\kappa', \qquad \boldsymbol{h}_1 = -\boldsymbol{v}, \qquad \boldsymbol{h}_2 = \frac{\kappa'}{\kappa^3}\boldsymbol{v}, \qquad \boldsymbol{h}_3 = -\frac{1}{\kappa^2}\boldsymbol{v}, \qquad \boldsymbol{m}_1 = -(\boldsymbol{m}\cdot\boldsymbol{n})\boldsymbol{v}, \qquad \boldsymbol{m}_2 = \frac{\boldsymbol{m}\cdot\boldsymbol{t}}{\kappa}\boldsymbol{v} - \frac{\boldsymbol{m}\cdot\boldsymbol{g}}{\kappa}\boldsymbol{t}. \tag{9.3}$$

The equation of equilibrium (8.25) on Edge I then becomes

$$-\Big(\frac{\mu l_2^2\,\kappa\kappa'}{4}\boldsymbol{v}\Big)' + \Big(\frac{\mu l_2\,\kappa}{2}\boldsymbol{u} - \frac{\mu l_2^2\kappa'^2}{4\kappa^2}\boldsymbol{v}\Big)'' - \Big(\frac{\mu l_2^2\kappa'}{4\kappa}\boldsymbol{v}\Big)''' + (\lambda\boldsymbol{t})' = \boldsymbol{s} - ((\boldsymbol{m}\cdot\boldsymbol{n})\boldsymbol{v})' + \Big(\frac{\boldsymbol{m}\cdot\boldsymbol{t}}{\kappa}\boldsymbol{v} - \frac{\boldsymbol{m}\cdot\boldsymbol{g}}{\kappa}\boldsymbol{t}\Big)'', \tag{9.4}$$

which, by (5.7) and (5.8), can be further written as

$$\Big(-\frac{3\mu l_2\kappa^2}{4} + \lambda\Big)'\boldsymbol{t} + \Big(\frac{\mu l_2\,(\kappa'' - \kappa^3)}{2} + \kappa\lambda\Big)\boldsymbol{u} - \frac{\mu l_2^2}{4}\Big(\frac{\kappa^2}{2} + \frac{\kappa''}{\kappa}\Big)''\boldsymbol{v} = \boldsymbol{s} - ((\boldsymbol{m}\cdot\boldsymbol{n})\boldsymbol{v})' + \Big(\frac{\boldsymbol{m}\cdot\boldsymbol{t}}{\kappa}\boldsymbol{v} - \frac{\boldsymbol{m}\cdot\boldsymbol{g}}{\kappa}\boldsymbol{t}\Big)''. \tag{9.5}$$

By the assumption that Edge I is traction-free and moment-free, the equilibrium equation yields three homogeneous scalar equations which, after eliminating $\lambda$, can be combined and reduced to a single scalar equation for the curvature $\kappa$ of the deformed edge:

$$2\kappa''(\alpha) + \kappa^3(\alpha) + c\kappa(\alpha) = 0, \qquad \alpha \in [0, l_1], \tag{9.6}$$

where $c$ is a constant. As might have been expected, (9.6) is the well-known equation for the curvature of a planar elastica. The solutions of (9.6), some of which were obtained by Euler (1744),[10] have been presented in numerous publications. Here, we present the solutions and the corresponding deformed configuration $S$ for the four subcases described above. A detailed discussion of the numerical solutions of a planar elastica can be found in a recent paper by Arroyo et al. (2020).

As a side note, the Lagrange multiplier $\lambda$ can be found from the equation of equilibrium (9.5) as

$$\lambda = -\frac{\mu l_2\,(\kappa'' - \kappa^3)}{2\kappa}. \tag{9.7}$$

As previously commented, $\lambda$ is an indeterminate part of the internal force in the direction of $\boldsymbol{t}$ on the edges that are under zero edge traction and zero edge moment.

### 9.1. Connecting edge placements and equal orientation tangent-normal vectors of Edges II and IV

In this subcase, Edges II and IV are clamped together in such a way that the tangent-normal vectors $\boldsymbol{g}$ to the two edges are aligned. We thus have the following edge placement and edge orientation conditions:

$$\tilde{\boldsymbol{y}}(0, x_2) = \tilde{\boldsymbol{y}}(l_1, x_2) \qquad \text{and} \qquad \boldsymbol{g}|_{x_1=0} = \boldsymbol{g}|_{x_1=l_1}. \tag{9.8}$$

Since

$$\left.\begin{aligned} \boldsymbol{d}(0) &= \tilde{\boldsymbol{y}}(0,0), \qquad \boldsymbol{d}(l_1) = \tilde{\boldsymbol{y}}(l_1,0),\\ \boldsymbol{d}'(0) &= \frac{\partial\tilde{\boldsymbol{y}}(x_1,x_2)}{\partial x_1}\Big|_{(x_1,x_2)=(0,0)} = \boldsymbol{g}|_{(x_1,x_2)=(0,0^+)},\\ \boldsymbol{d}'(l_1) &= \frac{\partial\tilde{\boldsymbol{y}}(x_1,x_2)}{\partial x_1}\Big|_{(x_1,x_2)=(l_1,0)} = -\boldsymbol{g}|_{(x_1,x_2)=(l_1,0^+)}, \end{aligned}\right\} \tag{9.9}$$

the edge conditions (9.8) imply that the spatial directrix $\boldsymbol{d}$ of Edge I must satisfy

$$\boldsymbol{d}(0) = \boldsymbol{d}(l_1) \qquad \text{and} \qquad \boldsymbol{d}'(0) = -\boldsymbol{d}'(l_1). \tag{9.10}$$

For non-constant $\kappa$, (9.6) can be integrated to yield the nonlinear first-order differential equation

$$4|\kappa'(\alpha)|^2 = -(\kappa^2(\alpha) - \kappa_0^2)(\kappa^2(\alpha) + \kappa_0^2 + 2c), \qquad \alpha \in [0, l_1], \tag{9.11}$$

where $\kappa_0$ is a constant corresponding to the maximum value of $\kappa$. The solutions of (9.11) can be expressed in terms of Jacobi elliptic functions. If, in particular, the parameters $c$ and $\kappa_0$ satisfy $2c + \kappa_0^2 > 0$ then the solution of (9.11) is given by

$$\kappa(\alpha) = \kappa_0 \cos\varphi(\alpha), \qquad \alpha \in [0, l_1], \tag{9.12}$$

[10] See Oldfather et al. (1933) for an annotated English translation of Euler's (1744) work on the elastica.

where $\varphi$ is the Jacobi amplitude function defined implicitly by

$$\alpha = \frac{l_1}{2} + \int_0^{\varphi} \frac{\mathrm{d}\vartheta}{q\sqrt{1 - p^2 \sin^2 \vartheta}}, \tag{9.13}$$

in which $p$ and $q$ are given by

$$p = \frac{\kappa_0}{\sqrt{2(\kappa_0^2 + c)}} \qquad \text{and} \qquad q = \sqrt{\frac{\kappa_0^2 + c}{2}}. \tag{9.14}$$

The spatial directrix of Edge I can be found by integrating the equations

$$|\boldsymbol{d}''(\alpha)| = \kappa(\alpha) \qquad \text{and} \qquad |\boldsymbol{d}'(\alpha)| = 1, \qquad \alpha \in [0, l_1]. \tag{9.15}$$

To this end, we define

$$\boldsymbol{e}_1 \equiv \frac{2\kappa'}{\kappa_0^2 + c}\boldsymbol{d}' - \frac{\kappa^2 + c}{(\kappa_0^2 + c)\kappa}\boldsymbol{d}'' \qquad \text{and} \qquad \boldsymbol{e}_2 \equiv \frac{\kappa^2 + c}{\kappa_0^2 + c}\boldsymbol{d}' + \frac{2\kappa'}{(\kappa_0^2 + c)\kappa}\boldsymbol{d}''. \tag{9.16}$$

It is readily verified from (9.6), (9.11), and (9.16) that $\boldsymbol{e}_1$ and $\boldsymbol{e}_2$ are fixed, orthonormal vectors. We can now write

$$\boldsymbol{d}'' = (\boldsymbol{d}''\cdot\boldsymbol{e}_1)\boldsymbol{e}_1 + (\boldsymbol{d}''\cdot\boldsymbol{e}_2)\boldsymbol{e}_2 = \frac{2\kappa''\boldsymbol{e}_1 + 2\kappa\kappa'\boldsymbol{e}_2}{\kappa_0^2 + c}. \tag{9.17}$$

Integrating (9.17) and using (9.11) and $(9.15)_2$, we find that

$$\boldsymbol{d}'(\alpha) = \frac{2\kappa'(\alpha)\boldsymbol{e}_1 + (\kappa^2(\alpha) + c)\boldsymbol{e}_2}{\kappa_0^2 + c}, \qquad \alpha \in [0, l_1], \tag{9.18}$$

and that

$$\begin{aligned}\boldsymbol{d}(\alpha) &= \frac{\kappa(\alpha)}{\kappa_0^2 + c}\boldsymbol{e}_1 + \int_0^{\alpha} \frac{\kappa_0^2\kappa^2(\alpha) + c}{\kappa_0^2 + c} d\alpha\, \boldsymbol{e}_2 \\ &= \frac{2\kappa_0 \cos\varphi(\alpha)}{\kappa_0^2 + c}\boldsymbol{e}_1 + \int_0^{\alpha} \frac{\kappa_0^2 \cos^2\varphi(\alpha) + c}{\kappa_0^2 + c} d\alpha\, \boldsymbol{e}_2, \qquad \alpha \in [0, l_1].\end{aligned} \tag{9.19}$$

The deformed surface $\mathcal{S}$ is given by

$$\tilde{\boldsymbol{y}}(x_1, x_2) = \boldsymbol{d}(x_1) + x_2\,\boldsymbol{e}_1 \times \boldsymbol{e}_2, \qquad x_1 \in [0, l_1],\ x_2 \in [0, l_2]. \tag{9.20}$$

It follows from (9.10) that the constant $c$ and $\kappa_0$ must satisfy

$$\int_0^{l_1} (\kappa_0^2 \cos^2\varphi(\alpha) + c)\,\mathrm{d}\alpha = 0 \qquad \text{and} \qquad c + \kappa_0^2 \cos\varphi(0) = 0. \tag{9.21}$$

For $l_1 = 1$, (9.13) and (9.21) admit a solution with the following numerical values of the parameters:

$$c = -36.7, \qquad \kappa_0 = 10.8. \tag{9.22}$$

The corresponding deformed surface $\mathcal{S}$ is depicted in Fig. 6. We note that (9.13) and (9.21) admit solutions other than (9.22), one of which corresponds, through (9.20), to a deformed surface whose connecting edges are pointing inwards. We conjecture that the deformed surface depicted in Fig. 6 corresponds to the most stable solution to (9.13) and (9.21) in the sense that it has the lowest bending energy among all possible competing solutions.

Induced by the edge orientation condition $(9.8)_2$ are two bending moments of equal magnitude and opposite direction on Edge II and IV, respectively. The magnitude $M$ of the bending moments is given by

$$M = \mu l_2 \kappa(0) = \mu l_2 \kappa(l_1). \tag{9.23}$$

It is found that $\kappa(0) = \kappa(l_1) = 6.01$ for the solution corresponding to (9.22).

### 9.2. Connecting edge placements and opposite orientation tangent-normal vectors of Edges II and IV

In this subcase, Edge II and IV are clamped together in such a way that the tangent-normal vectors $\boldsymbol{g}$ to the two edges are opposite to each other. We thus have the following edge placement and edge orientation conditions:

$$\tilde{\boldsymbol{y}}(0, x_2) = \tilde{\boldsymbol{y}}(l_1, x_2) \qquad \text{and} \qquad \boldsymbol{g}|_{x_1=0} = -\boldsymbol{g}|_{x_1=l_1}. \tag{9.24}$$

By the same argument that led to (9.10), the edge conditions (9.24) imply that the spatial directrix $\boldsymbol{d}(\alpha)$ of Edge I must satisfy

$$\boldsymbol{d}(0) = \boldsymbol{d}(l_1) \qquad \text{and} \qquad \boldsymbol{d}'(0) = \boldsymbol{d}'(l_1). \tag{9.25}$$

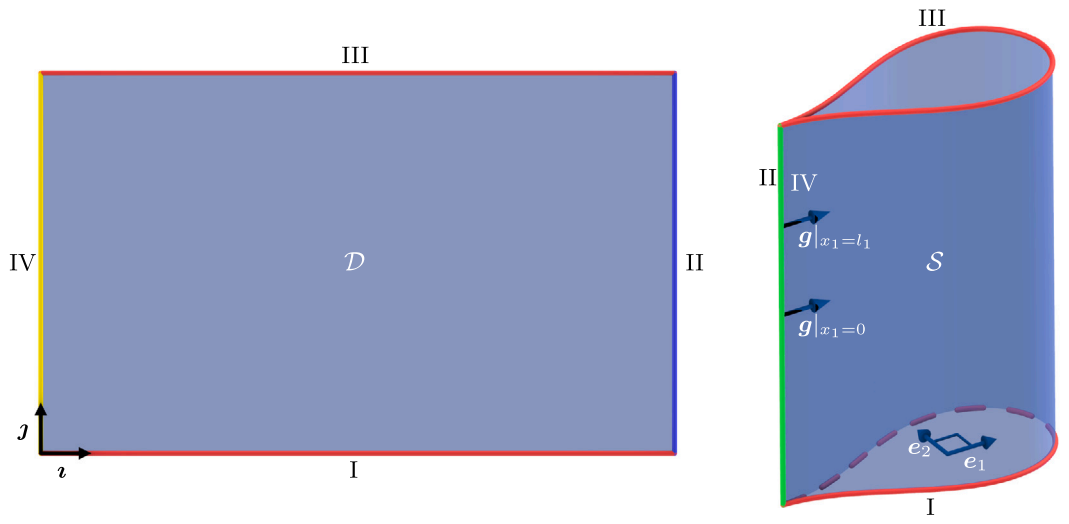


**Fig. 6.** Left: Rectangular reference configuration $\mathcal{D}$. Right: Cuspoidal cylindrical equilibrium configuration $\mathcal{S}$ corresponding to the deformation $\tilde{\boldsymbol{y}}$, as defined in (9.20), determined by clamping Edges II and IV by applying edge placements $(9.8)_1$ and equal orientation tangent-normal edge vectors $(9.8)_2$.

Under these conditions, the deformed surface is a circular cylinder as expected. Specifically, the solution of (9.6) corresponds to constant curvature

$$\kappa(\alpha) = \frac{2\pi}{l_1}, \qquad \alpha \in [0, l_1]. \tag{9.26}$$

The spatial directrix of Edge I can be found by integrating (9.15) subject to the boundary condition (9.25), yielding

$$\boldsymbol{d}(\alpha) = \frac{l_1}{2\pi}\left(\cos\frac{2\pi\alpha}{l_1}\,\boldsymbol{e}_1 + \sin\frac{2\pi\alpha}{l_1}\,\boldsymbol{e}_2\right), \tag{9.27}$$

where $\boldsymbol{e}_1$ and $\boldsymbol{e}_2$ are again orthonormal.

The deformed surface $\mathcal{S}$ is again given by

$$\tilde{\boldsymbol{y}}(x_1, x_2) = \boldsymbol{d}(x_1) + x_2\,\boldsymbol{e}_1 \times \boldsymbol{e}_2, \qquad x_1 \in [0, l_1],\ x_2 \in [0, l_2] \tag{9.28}$$

and is depicted in Fig. 7.

Again, certain bending moments $M_b$, given by (9.23), are induced by the edge orientation condition $(9.24)_2$ on Edge II and IV. As a comparison of Subcases 1 and 2, we take $l_1 = 1$ and note from (9.26) that $\kappa(0) = \kappa(l_1) = 2\pi$, while $\kappa(0) = \kappa(l_1) = 6.01$ in Subcase 1. However, the directions of the bending moments are oppositely directed in these two subcases. These bending moments are applied by the devices that impose the edge conditions (9.8) and (9.24) in Subcases 1 and 2. We also note a more subtle difference: The connecting edge placement condition $(9.8)_1$ in Subcase 1 must be companied by two forces on the edges, while the connecting edge placement condition $(9.24)_1$ is satisfied under zero edge force. Indeed, as shall be seen in the next subsection, the prescribed edge bending moments alone deform the material surface into a right circular cylinder depicted in Fig. 7.

We also note that the expression for the Lagrange multiplier $\lambda$ in (9.7) reduces, for the current Subcase 2 and the next Subcase 3, to

$$\lambda = \frac{2\pi^2\mu l_2}{l_1^2}. \tag{9.29}$$

### *9.3. No placement and orientation edge conditions with constant moments on Edges II and IV*

The analysis of this subcase serves a two-fold purpose. First, it shows that the deformation in the Subcase 2 can be obtained by replacing the edge placement and orientation conditions with the appropriate edge tractions and edge moments on Edges II and IV. Secondly, it demonstrates a method to treat the special cases where the directrix and a generatrix coincide.

We assign, instead of the edge placement and edge orientation (9.24), the following edge tractions and edge moments on Edges II and IV

$$\boldsymbol{s} = \boldsymbol{0} \qquad \text{and} \qquad \boldsymbol{m} = m\boldsymbol{t}, \tag{9.30}$$

where $m$ is a constant bending moment and $\boldsymbol{t}$ is again the unit tangent vector along the deformed Edges II and IV. Note that the bending moments on Edges II and IV are of equal magnitude but opposite orientation.

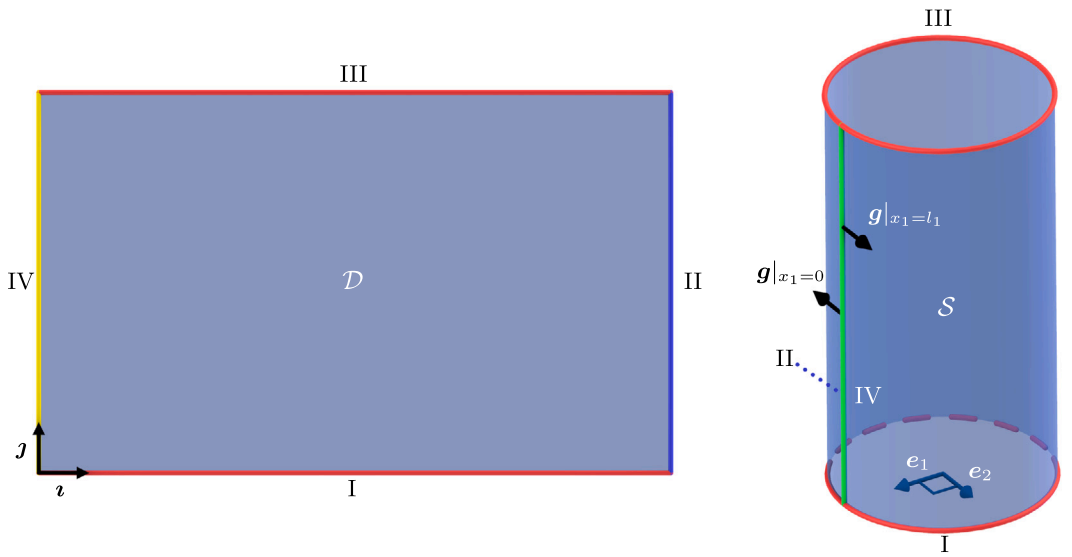


**Fig. 7.** Left: Rectangular reference configuration $\mathcal{D}$. Right: Right-circular cylindrical equilibrium configuration $\mathcal{S}$ corresponding to the deformation $\tilde{\boldsymbol{y}}$, as defined in (9.28), determined by clamping Edges II and IV through the application of edge placements $(9.24)_1$ and oppositely oriented tangent-normal edge vectors $(9.24)_2$.

A side note here is that although we have assigned the edge placement and edge orientation conditions (9.24) in Subcase 2, and we have assigned the edge traction and edge moment (9.30) in the current Subcase 3, nothing can prevent us from assigning both edge loads (9.30) and the edge placement and edge orientation conditions (9.24) simultaneously. If that is done, then the assignment of the edge loads (9.30) has no effect on the deformation of the material surface, and the same solution as in the Subcase 2 prevails. As previously discussed, the edge loads influence the deformation only through their appearance in the equation of equilibrium (8.25), which is derived and is valid only on the portion of an edge where the placement is not prescribed.

Although the edge placement is not prescribed in the current Subcase 3, we encounter the situation where the equation of equilibrium (8.25) does not hold on Edges II and IV for a different reason. Namely, it is due to the degeneracy that arises from the coincidence of the directrices and generatrices on Edges II and IV. In the parametrizations (2.2) for the referential and spatial surfaces $\mathcal{D}$ and $\mathcal{S}$, it is required that the directrices and the generatrices do not coincide. A possible remedy for treating this degeneracy is to use a perturbation analysis in which Edges II and IV are infinitesimally altered in such a way that the perturbed directrix and generatrix do not coincide, and that the desired results are obtained as the limit of zero perturbation. Such an analysis, while sufficient to handle the degeneracy, generally involves substantial computations.

In this work, we present an alternative approach to a perturbation analysis of the kind just described. This alternative approach is based on the idea of taking a special kinematically admissible virtual displacement $\delta\boldsymbol{d}$ for the entirety of Edges II and IV.

Since the directrix and generatrix coincide on Edge II, we have

$$\boldsymbol{d}(\alpha) = \boldsymbol{d}(l_1) + (\alpha - l_1)\boldsymbol{e}(l_1), \qquad \alpha \in [l_1, l_1 + l_2]. \tag{9.31}$$

An examination of the expression for the bending energy functional $E_{\mathcal{S}}$ in (7.2) reveals that the area element associated with Edge II is zero since $\hat{\boldsymbol{y}}_{,\alpha} = \hat{\boldsymbol{y}}_{,\beta} = \boldsymbol{e}(l_1)$, and therefore there is no contribution to the bending energy (7.11) in the interval $\alpha \in [l_1, l_1 + l_2]$. On the other hand, the virtual work of the edge traction $\boldsymbol{s}$ and the edge moment $\boldsymbol{m}$ on the right-hand side of (8.13) need not vanish when the entire Edge II has a virtual displacement in which the directrix and the generatrix remain coincident. By (9.31), we have on Edge II the relations

$$\left.\begin{aligned} &\boldsymbol{t}(\alpha) = \boldsymbol{d}'(\alpha) = \boldsymbol{e}(l_1), \qquad \boldsymbol{g}(\alpha) = \boldsymbol{n}(\alpha)\times\boldsymbol{t}(\alpha) = \boldsymbol{n}(l_1)\times\boldsymbol{e}(l_1), \qquad \boldsymbol{n}(\alpha) = \boldsymbol{n}(l_1),\\ &\delta\boldsymbol{d}(\alpha) = \delta\boldsymbol{d}(l_1) + (\alpha - l_1)\delta\boldsymbol{e}(l_1), \qquad \delta\boldsymbol{t}(\alpha) = \delta\boldsymbol{e}(l_1). \end{aligned}\right\} \tag{9.32}$$

Here, we have used the fact that the normal vector $\boldsymbol{n}$ is continuous at the corner of Edges I and II, and it remains constant along a generator and therefore along Edge II. The virtual work of the edge loads can then be expressed as

$$\begin{aligned} &\int_{l_1}^{l_1+l_2} (\boldsymbol{s}\cdot\delta\boldsymbol{d} + \boldsymbol{m}\cdot((\boldsymbol{n}\cdot\delta\boldsymbol{g})\boldsymbol{t} + (\boldsymbol{t}\cdot\delta\boldsymbol{n})\boldsymbol{g} + (\boldsymbol{g}\cdot\delta\boldsymbol{t})\boldsymbol{n}))\,\mathrm{d}\alpha\\ &\quad= \int_{l_1}^{l_1+l_2} \big(\boldsymbol{s}\cdot(\delta\boldsymbol{d}(l_1) + (\alpha - l_1)\delta\boldsymbol{e}(l_1)) - (\boldsymbol{m}\cdot\boldsymbol{t})(\boldsymbol{n}(l_1)\times\boldsymbol{e}(l_1))\cdot\delta\boldsymbol{n}(l_1) + (\boldsymbol{m}\cdot\boldsymbol{g})\boldsymbol{e}(l_1)\cdot\delta\boldsymbol{n}(l_1) + (\boldsymbol{m}\cdot\boldsymbol{n})(\boldsymbol{n}(l_1)\times\boldsymbol{e}(l_1))\cdot\delta\boldsymbol{e}(l_1)\big)\,\mathrm{d}\alpha\\ &\quad= \overline{\boldsymbol{s}}\cdot\delta\boldsymbol{d}(l_1) + \overline{\boldsymbol{s}_1}\cdot\delta\boldsymbol{e}(l_1) - \overline{m_t}(\boldsymbol{n}(l_1)\times\boldsymbol{e}(l_1))\cdot\delta\boldsymbol{n}(l_1) + \overline{m_g}\boldsymbol{e}(l_1)\cdot\delta\boldsymbol{n}(l_1) + \overline{m_n}(\boldsymbol{n}(l_1)\times\boldsymbol{e}(l_1))\cdot\delta\boldsymbol{e}(l_1), \end{aligned} \tag{9.33}$$

where $\overline{\boldsymbol{s}}$, $\overline{\boldsymbol{s}_1}$, $\overline{m_t}$, $\overline{m_g}$, and $\overline{m_n}$ are defined by

$$\left.\begin{aligned} \overline{\boldsymbol{s}} &\equiv \int_{l_1}^{l_1+l_2} \boldsymbol{s}\,\mathrm{d}\alpha, \qquad \overline{\boldsymbol{s}_1} \equiv \int_{l_1}^{l_1+l_2} (\alpha - l_1)\boldsymbol{s}\,\mathrm{d}\alpha, \\ \overline{m_t} &\equiv \int_{l_1}^{l_1+l_2} \boldsymbol{m}\cdot\boldsymbol{t}\,\mathrm{d}\alpha, \qquad \overline{m_g} \equiv \int_{l_1}^{l_1+l_2} \boldsymbol{m}\cdot\boldsymbol{g}\,\mathrm{d}\alpha, \qquad \text{and} \qquad \overline{m_n} \equiv \int_{l_1}^{l_1+l_2} \boldsymbol{m}\cdot\boldsymbol{n}\,\mathrm{d}\alpha. \end{aligned}\right\} \tag{9.34}$$

We denote the virtual work of the edge loads on Edge II by

$$W_{\mathrm{II}} \equiv \overline{\boldsymbol{s}}\cdot\delta\boldsymbol{d}(l_1) + \overline{\boldsymbol{s}_1}\cdot\delta\boldsymbol{e}(l_1) - \overline{m_t}(\boldsymbol{n}(l_1)\times\boldsymbol{e}(l_1))\cdot\delta\boldsymbol{n}(l_1) + \overline{m_g}\boldsymbol{e}(l_1)\cdot\delta\boldsymbol{n}(l_1) + \overline{m_n}(\boldsymbol{n}(l_1)\times\boldsymbol{e}(l_1))\cdot\delta\boldsymbol{e}(l_1). \tag{9.35}$$

The variational problem (8.19) now becomes

$$\int_{[0,l_1]\cup[l_1+l_2,2l_1+l_2]} (\delta(F-\lambda(|\boldsymbol{d}'|-1)) - \boldsymbol{s}\cdot\delta\boldsymbol{d} - \boldsymbol{m}\cdot((\boldsymbol{n}\cdot\delta\boldsymbol{g})\boldsymbol{t} - (\boldsymbol{t}\cdot\delta\boldsymbol{n})\boldsymbol{g} - (\boldsymbol{g}\cdot\delta\boldsymbol{t})\boldsymbol{n}))\,\mathrm{d}\alpha = W_{\mathrm{II}} + W_{\mathrm{IV}}, \tag{9.36}$$

where $W_{\mathrm{IV}}$ is the virtual work of the edge loads on Edge IV, defined by (9.34) and (9.35), with obvious replacement of $l_1$ by $2l_1+l_2$, and of $l_1+l_2$ by $2l_1+2l_2$. By the same analysis presented in Section 8 we again obtain the equation of equilibrium (8.25) and the jump conditions (8.26) and (8.28)–(8.30), which must hold on Edges I and III. In addition, by considering variations $\delta\boldsymbol{d}$ that vanish on Edges I and III except near the corner points $\alpha=0$, $\alpha=l_1$, $\alpha=l_1+l_2$, and $\alpha=2l_1+l_2$ and that leave Edges II and IV remaining to be the coinciding directrix and generatrix, we obtain the following corner conditions that must hold at $\alpha=0$, $\alpha=l_1$, $\alpha=l_1+l_2$, and $\alpha=2l_1+l_2$:

$$\left.\begin{aligned} (\boldsymbol{I}-\boldsymbol{t}\otimes\boldsymbol{t})\Big(2B\boldsymbol{h}_1 - 2\Big(\frac{\partial F}{\partial\kappa}\boldsymbol{u} + B\boldsymbol{h}_2\Big)' + (2B\boldsymbol{h}_3)'' - 2\lambda\boldsymbol{d}' + 2\boldsymbol{m}_1 + 2\boldsymbol{m}_2' - \overline{\boldsymbol{s}}\Big) &= \boldsymbol{0}, \\ (\boldsymbol{I}-\boldsymbol{t}\otimes\boldsymbol{t})\Big(2\frac{\partial F}{\partial\kappa}\boldsymbol{u} + 2B\boldsymbol{h}_2 - (2B\boldsymbol{h}_3)' - 2\boldsymbol{m}_2 - \cos\theta(\overline{\boldsymbol{s}_1} + \overline{m_n}\boldsymbol{n}\times\boldsymbol{e}) - \sin\theta(\overline{\boldsymbol{s}_1}\times\boldsymbol{n} + \overline{m_n}\boldsymbol{e}) \\ - \cos\phi(\overline{m_t}\boldsymbol{n}\times\boldsymbol{e} - \overline{m_g}\boldsymbol{e})\times\boldsymbol{u} - \sin\phi(\overline{m_t}\sin\theta + \overline{m_g}\cos\theta)\boldsymbol{u}\Big) &= \boldsymbol{0}, \\ \frac{2\sin^2\theta}{\kappa\sin\phi}B + \overline{\boldsymbol{s}_1}\cdot\boldsymbol{n} + \overline{m_t}\cos\theta - \overline{m_g}\sin\theta &= 0. \end{aligned}\right\} \tag{9.37}$$

The factor of two in (9.37) arises because a virtual displacement of Edge II (or Edge IV) is companied by appropriate virtual displacements of the two end points of Edges I and III. We note that the corner conditions (9.37) are valid only when the directrix and the generatrix coincide on a part of the edge.

For the edge loads in the current Subcase 3, we have $\overline{\boldsymbol{s}_1}=\boldsymbol{0}$, $\overline{m_t}=ml_2$, and $\overline{m_g}=\overline{m_n}=0$ on Edges II and IV. It then follows from $(9.37)_2$ that

$$\mu l_2\kappa\boldsymbol{u} - \frac{\mu l_2^2\kappa'^2}{2\kappa^2}\boldsymbol{v} - \Big(\frac{\mu l_2^2\kappa'}{2\kappa}\Big)'\boldsymbol{v} - ml_2\boldsymbol{u} = \boldsymbol{0}, \qquad \alpha = 0,\ l_1,\ l_1+l_2,\ 2l_1+l_2. \tag{9.38}$$

Here we have made use of (9.3) and the conditions $\phi=\theta=\pi/2$. The components of (9.38) give

$$\kappa(0) = \kappa(l_1) = \frac{m}{\mu} \qquad \text{and} \qquad \kappa''(0) = \kappa''(l_1) = 0, \tag{9.39}$$

which, in combination with (9.6) lead to

$$\kappa(\alpha) = \frac{m}{\mu}, \qquad \alpha\in[0,l_1]. \tag{9.40}$$

Therefore, the deformed surface is a partial circular cylinder with radius $\mu/m$. For the special value of the bending moment $m=2\pi\mu/l_1$, the cylinder closes, and the resulting deformation is identical to that in the Subcase 2, given by (9.27) and (9.28), as depicted in Fig. 8. Recalling $(9.30)_2$, we see that the assigned edge moments $\boldsymbol{m}$ are vectors in the directions of $\boldsymbol{t}$ and hence are bending moments as indicated by the curved arrows in Fig. 8. Furthermore, the magnitude of $\boldsymbol{m}$ as defined is the moment per unit edge length. Therefore, it follows from $(9.38)_1$ that the magnitude $M$ of the total bending moment on Edge II is $M=l_2m=\mu l_2\kappa(l_1)$ while that on Edge IV is $M=\mu l_2\kappa(0)$. This also provides a justification of (9.23).

We note that since $\kappa$ is constant on Edges I and III in this subcase, $(9.3)_2$ gives $B=0$. Therefore, the two remaining corner conditions $(9.37)_{1,3}$ are satisfied automatically.

In this subcase, the expression for the Lagrange multiplier $\lambda$ is given by (9.29).

### 9.4. Connecting edge placements and zero edge loads on Edges II and IV

In this subcase, a mixed edge condition is assigned. Specifically, we prescribe the connecting edge placement condition

$$\tilde{\boldsymbol{y}}(0,x_2) = \tilde{\boldsymbol{y}}(l_1,x_2) \tag{9.41}$$

and the (zero) edge moment condition

$$\boldsymbol{m} = \boldsymbol{0}. \tag{9.42}$$

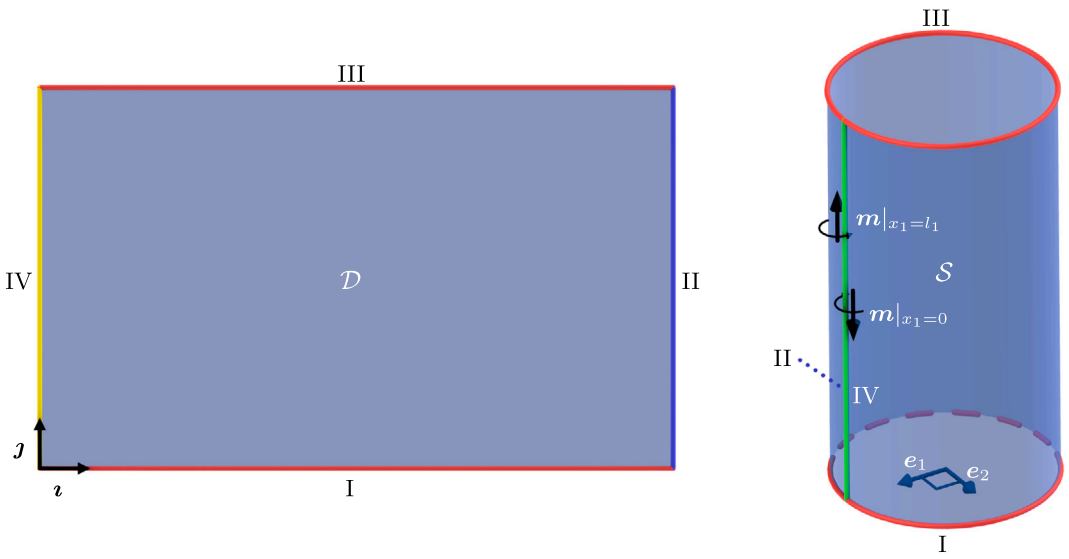


**Fig. 8.** Left: Rectangular reference configuration $\mathcal{D}$. Right: Right-circular cylindrical equilibrium configuration $\mathcal{S}$ determined by the application of (zero) edge tractions $(9.30)_1$ and (non-zero) edge moments $(9.30)_2$ to Edges II and IV. In this case and granted that $m = 2\pi\mu/l_1$ (so that the cylinder is closed), the deformation $\tilde{\boldsymbol{y}}$ is identical to that defined in (9.28).

The connecting edge placement conditions (9.41) again requires that

$$\boldsymbol{d}(0) = \boldsymbol{d}(l_1) \tag{9.43}$$

on Edge I. On the other hand, the zero edge moment (9.42) implies that

$$\kappa(0) = \kappa(l_1) = 0 \qquad \text{and} \qquad \kappa''(0) = \kappa''(l_1) = 0. \tag{9.44}$$

These conditions follow from the same analysis as that leading to (9.39) in Subcase 3.

The form of the solution $\kappa$ of (9.6) is the same as that in Subcase 1 with $(9.21)_2$ being replaced by a new equation. Specifically, the curvature of the deformed Edge I is given by

$$\kappa(\alpha) = \kappa_0 \cos\varphi(\alpha), \qquad \alpha \in [0, l_1], \tag{9.45}$$

where $\varphi$ is again the Jacobi amplitude function defined by (9.13) and (9.14). The spatial directrix of Edge I is given by

$$\boldsymbol{d}(\alpha) = \frac{2\kappa_0 \cos\varphi(\alpha)}{\kappa_0^2 + c}\boldsymbol{e}_1 + \int_0^\alpha \frac{\kappa_0^2 \cos^2\varphi(\alpha) + c}{\kappa_0^2 + c} d\alpha\, \boldsymbol{e}_2, \qquad \alpha \in [0, l_1], \tag{9.46}$$

and the deformed surface $\mathcal{S}$ is given by

$$\tilde{\boldsymbol{y}}(x_1, x_2) = \boldsymbol{d}(x_1) + x_2 \boldsymbol{e}_1 \times \boldsymbol{e}_2, \qquad x_1 \in [0, l_1],\ x_2 \in [0, l_2]. \tag{9.47}$$

It follows from (9.43) and (9.44) that the constant $c$ and $\kappa_0$ must satisfy

$$\int_0^{l_1} (\kappa_0^2 \cos^2\varphi(\alpha) + c)\, \mathrm{d}\alpha = 0 \qquad \text{and} \qquad \cos\varphi(0) = 0. \tag{9.48}$$

We note that an additional provision, namely $(9.48)_2$, is required to satisfy the conditions (9.44).

For $l_1 = 1$, (9.13), (9.14), and (9.48) admit a solution with the following numerical values of the parameters:

$$c = -28.1, \qquad \kappa_0 = 8.44. \tag{9.49}$$

The corresponding deformed surface $\mathcal{S}$ is depicted in Fig. 9.

A comparison of Subcases 1 and 4 reveals the effects of the different edge conditions on the deformed surface. In Subcase 1, the edge orientations are as prescribed in $(9.8)_2$. Consequently, appropriate bending moments must be applied to the edges by the device that prescribe the edge orientation. In Subcase 4, on the other hand, the (zero) edge moments are imposed by (9.42) and the edge orientations are not prescribed. The resulting solution subsequently gives the edge orientations as indicated in Fig. 9.

We also note that it follows from (9.45) and $(9.48)_2$ that $\kappa(0) = \kappa(l_1) = 0$, and, therefore, that $B(0) = B(l_1) = 0$ by $(9.3)_2$. This ensures that the corner conditions $(9.37)_{1,3}$ are once again satisfied automatically.

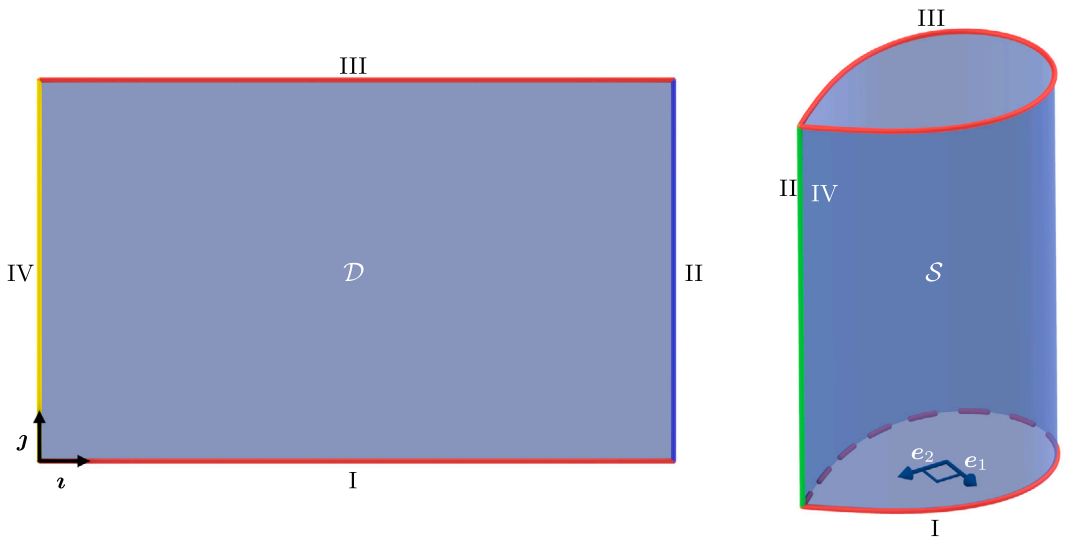


**Fig. 9.** Left: Rectangular reference configuration $\mathcal{D}$. Right: Cornered cylindrical equilibrium configuration $\mathcal{S}$ corresponding to the deformation $\bar{\mathbf{y}}$, as defined in (9.47), determined by connecting Edges II and IV by applying edge placements (9.41) and (zero) edge moments (9.42).

## 10. Summary

We have developed a general framework for determining the equilibrium shape of an inextensional material surface of general geometry that deforms under prescribed boundary conditions of edge placements, dead-load edge tractions, and dead-load edge moments. Apart from being flat, the undistorted reference configuration of the material surface is essentially unrestricted. In particular, the reference shape is not limited to being ribbon-like in the sense that its width in some direction is small relative to its width in some other direction. Our theory is based on a representation of an isometric deformation, from a flat surface to a developable surface, in terms of a collection of straight-line generators in $\mathcal{E}^3$ together with an appropriately designated space curve, called the spatial directrix, through which the field of generators uniquely intersect. For our analysis, we select the edge of the material surface as the directrix. This previously unexplored choice ensures satisfaction of the covering requirement that, for any isometric deformation of $\mathcal{D}$, each material point is passed by a generator, and thus leads to the complete class of isometric deformations that are possible for a general reference configuration. Other approaches which select a directrix that is internal to the material surface, such as the midline for a rectangular reference strip, generally violate the covering requirement, making it impossible to ensure that each point on the deformed image of the strip is unambiguously identified with a material point corresponding to a fixed position in the reference strip.

An advantage of our strategy is that a dimensional reduction of the total bending energy can be accomplished in closed form while avoiding any approximation associated with partial covering. We formalize this idea and develop a faithful dimensional reduction of the total bending energy by performing an integration along the generators, leading to a one-dimensional variational problem to determine the equilibrium configuration of the material surface. The resulting bending energy integral is a functional of the spatial directrix, which by our choice corresponds to the edge of the deformed surface. To complete the formulation of the variational problem based on the principle of virtual work, we write the potential energy of the dead-load edge tractions as a functional of the spatial directrix. Furthermore, the work done by the dead-load edge moments through an isometric infinitesimal surface deformation at the edge is shown to be a functional of the variations of the derivatives of the spatial directrix.

We then derive the Euler–Lagrange equation and jump conditions associated with the functional of the bending energy and the work done by the edge loads, which is an essential logical step in the variational characterization of equilibrium, but has not been previously done, notwithstanding that it was implied by Sadowsky (1930) more than 80 years ago. A major consequence of the dimensional reduction of the energy functional is that the resulting Euler–Lagrange equation is an ordinary differential equation for the spatial directrix. Any solution to this equation determines the equilibrium image of the edge of the deformed surface, and thus the equilibrium configuration of the deformed surface. The edge traction and edge moment enter the equation directly. To illustrate the range of applicability of our framework, we present an example of the equilibrium shapes of a rectangular strip under various edge conditions.

## Declaration of competing interest

The authors declare that they have no known competing financial interests or personal relationships that could have appeared to influence the work reported in this paper.

## Data availability

No data was used for the research described in the article.

## Acknowledgments

We thank the reviewers for their constructive input which added clarity and led to improvements in our presentation. We also thank Michael Grunwald for his expert help with preparing the figures. Eliot Fried gratefully acknowledges support from the Okinawa Institute of Science and Technology Graduate University with subsidy funding from the Cabinet Office, Government of Japan. Yi-chao Chen thanks the Okinawa Institute of Science and Technology for hospitality and generous support during a sabbatical and subsequent visits.

## Appendix A. Variations

In this Appendix, we obtain expressions for the variations of the intermediate variables $\kappa$, $\theta$, $\bar{\alpha}$, $\bar{\beta}$, and $\boldsymbol{n}$ in terms of $\delta\boldsymbol{d}'$, $\delta\boldsymbol{d}''$, and $\delta\boldsymbol{d}'''$. As noted in Section 8, these variations are required to derive the first variation of the energy functional with respect to the independent variable $\boldsymbol{d}$ and, thus, to derive the Euler–Lagrange equation (8.25).

From the definitions $(5.1)_2$ and (5.3) of the unit normal and curvature $\kappa$ of the spatial directrix, we see that $\delta\kappa$ is given in terms of $\delta\boldsymbol{d}''$ by

$$\delta\kappa = \frac{\boldsymbol{d}''\cdot\delta\boldsymbol{d}''}{|\boldsymbol{d}''|} = \boldsymbol{u}\cdot\delta\boldsymbol{d}''. \tag{A.1}$$

Toward finding $\delta\theta$, we first take the variation of (4.4) to find that $\delta\phi$ and $\delta\phi'$ are given in terms of $\delta\kappa$ and $\delta\kappa'$ by

$$\delta\phi = \frac{\cot\phi}{\kappa}\delta\kappa \qquad \text{and} \qquad \delta\phi' = -\frac{\kappa\phi'\csc^2\phi + \kappa'\cot\phi}{\kappa^2}\delta\kappa + \frac{\cot\phi}{\kappa}\delta\kappa'. \tag{A.2}$$

Varying (4.5) while using (5.1) and (5.3), we next find that $\delta\tau$ is given in terms of $\delta\boldsymbol{d}'$, $\delta\boldsymbol{d}''$, and $\delta\boldsymbol{d}'''$ by

$$\delta\tau = (\tau\boldsymbol{t} + \kappa\boldsymbol{v})\cdot\delta\boldsymbol{d}' - \frac{\kappa\tau\boldsymbol{u} + \kappa'\boldsymbol{v}}{\kappa^2}\cdot\delta\boldsymbol{d}'' + \frac{\boldsymbol{v}}{\kappa}\cdot\delta\boldsymbol{d}'''. \tag{A.3}$$

Varying (4.3) and using (A.1)–(A.3) along with (5.7), we find that $\delta\theta$ also depends on $\delta\boldsymbol{d}'$, $\delta\boldsymbol{d}''$, and $\delta\boldsymbol{d}'''$ and is given by

$$\begin{aligned}\delta\theta &= \frac{\sin\theta\cos\theta(\sin\phi\,\delta\kappa + \kappa\cos\phi\,\delta\phi) - \sin^2\theta(\delta\tau + \delta\phi')}{\kappa\sin\phi}\\ &= -\frac{\sin^2\theta}{\kappa\sin\phi}(\tau\boldsymbol{t} + \kappa\boldsymbol{v})\cdot\delta\boldsymbol{d}' + \frac{\sin^2\theta}{\kappa\sin^2\phi}\Big(\cos\phi\,\boldsymbol{t} + 2\cot\theta\,\boldsymbol{u} + \frac{\kappa' - \kappa\tau\cot\phi}{\kappa^2}\boldsymbol{g}\Big)\cdot\delta\boldsymbol{d}'' - \frac{\sin^2\theta}{\kappa^2\sin^2\phi}\boldsymbol{g}\cdot\delta\boldsymbol{d}'''.\end{aligned} \tag{A.4}$$

We next show that $\delta\bar{\alpha}$ and $\delta\bar{\beta}$ are both proportional to $\delta\theta$ and, thus, by (A.4), can be expressed in terms of $\delta\boldsymbol{d}'$, $\delta\boldsymbol{d}''$, and $\delta\boldsymbol{d}'''$. Varying the representation (4.1) for the referential generatrix $\boldsymbol{b}$, we see that $\delta\boldsymbol{b}$ is given by

$$\delta\boldsymbol{b} = \boldsymbol{b}^\perp\delta\theta, \tag{A.5}$$

where $\boldsymbol{b}^\perp$ is defined by

$$\boldsymbol{b}^\perp \equiv -\sin\theta\,\boldsymbol{a}' + \cos\theta\,\boldsymbol{\jmath}. \tag{A.6}$$

Varying (8.23), which determines both $\bar{\alpha}$ and $\bar{\beta}$, we see that

$$\boldsymbol{a}'(\bar{\alpha})\delta\bar{\alpha} = \delta\bar{\beta}\,\boldsymbol{b} + \bar{\beta}\delta\boldsymbol{b}. \tag{A.7}$$

Resolving (A.7) in the directions of $\boldsymbol{b}$ and $\boldsymbol{b}^\perp$ and using (A.5), we see further that

$$\boldsymbol{b}\cdot\boldsymbol{a}'(\bar{\alpha})\delta\bar{\alpha} = \delta\bar{\beta} \qquad \text{and} \qquad \boldsymbol{b}^\perp\cdot\boldsymbol{a}'(\bar{\alpha})\delta\bar{\alpha} = \bar{\beta}\boldsymbol{b}^\perp\cdot\delta\boldsymbol{b} = \bar{\beta}\delta\theta \tag{A.8}$$

and, thus, by (A.8), that $\delta\bar{\alpha}$ and $\delta\bar{\beta}$ can be expressed as

$$\delta\bar{\alpha} = \frac{\bar{\beta}}{\boldsymbol{b}^\perp\cdot\boldsymbol{a}'(\bar{\alpha})}\delta\theta \qquad \text{and} \qquad \delta\bar{\beta} = \frac{\bar{\beta}\boldsymbol{b}\cdot\boldsymbol{a}'(\bar{\alpha})}{\boldsymbol{b}^\perp\cdot\boldsymbol{a}'(\bar{\alpha})}\delta\theta. \tag{A.9}$$

Recognizing that the variations in (A.9) can be written in alternative forms with $\theta(\bar{\alpha})$ being defined through

$$\cos\theta(\bar{\alpha}) = \boldsymbol{b}(\bar{\alpha})\cdot\boldsymbol{a}'(\bar{\alpha}) \tag{A.10}$$

while bearing in mind that $\boldsymbol{b}(\bar{\alpha}) = -\boldsymbol{b}(\alpha)$, we see that (A.9) can be expressed alternatively as

$$\delta\bar{\alpha} = \bar{\beta}\csc\theta(\bar{\alpha})\delta\theta \qquad \text{and} \qquad \delta\bar{\beta} = -\bar{\beta}\cot\theta(\bar{\alpha})\delta\theta. \tag{A.11}$$

Finally, varying $\boldsymbol{n}$ in (5.7) and invoking $(5.1)_{2,3}$, (A.1), and $(A.2)_1$, we see that $\delta\boldsymbol{n}$ is given in terms of $\delta\boldsymbol{d}'$ and $\delta\boldsymbol{d}''$ by

$$\begin{aligned}\delta\boldsymbol{n} &= -(\cos\phi\,\boldsymbol{u} + \sin\phi\,\boldsymbol{v})\delta\phi - \sin\phi\,\delta\boldsymbol{u} + \cos\phi\,\delta\boldsymbol{v}\\ &= -\cos\phi\,\boldsymbol{u}\times\delta\boldsymbol{d}' - \Big(\frac{\sin\phi}{\kappa}\boldsymbol{t}\otimes\boldsymbol{t} + \frac{1}{\kappa\sin\phi}\boldsymbol{g}\otimes\boldsymbol{g}\Big)\delta\boldsymbol{d}''.\end{aligned} \tag{A.12}$$

## Appendix B. Jump conditions

In this Appendix, we derive the jump conditions (8.28) arising from the requirement (8.27) that the components of $\delta\boldsymbol{d}'$ be continuous relative to the Darboux frame $\{\boldsymbol{t},\boldsymbol{g},\boldsymbol{n}\}$.

We begin by using the Euler–Lagrange equation (8.25) and the jump condition (8.26) to reduce the first variation condition (8.21), giving:

$$\left[\!\!\left[\Big(\frac{\partial F}{\partial\kappa}\boldsymbol{u}+\frac{\partial F}{\partial\theta'}\boldsymbol{h}_1+B\boldsymbol{h}_2-(B\boldsymbol{h}_3)'-\boldsymbol{m}_2\Big)\cdot\delta\boldsymbol{d}'+\Big(\frac{\partial F}{\partial\theta'}\boldsymbol{h}_2+B\boldsymbol{h}_3\Big)\cdot\delta\boldsymbol{d}''+\frac{\partial F}{\partial\theta'}\boldsymbol{h}_3\cdot\delta\boldsymbol{d}'''\right]\!\!\right]=0. \tag{B.1}$$

Then, using the consequences

$$\boldsymbol{d}'\cdot\delta\boldsymbol{d}'=0,\qquad \boldsymbol{d}''\cdot\delta\boldsymbol{d}'+\boldsymbol{d}'\cdot\delta\boldsymbol{d}''=0,\qquad \boldsymbol{d}'''\cdot\delta\boldsymbol{d}'+2\boldsymbol{d}''\cdot\delta\boldsymbol{d}''+\boldsymbol{d}'\cdot\delta\boldsymbol{d}'''=0, \tag{B.2}$$

of the constraint $(2.4)_4$ in (B.1) and invoking the conditions (8.27) ensuring that the components of $\delta\boldsymbol{d}'$ are continuous relative to the Darboux frame $\{\boldsymbol{t},\boldsymbol{g},\boldsymbol{n}\}$, we find that

$$\begin{aligned}
0&=\left[\!\!\left[\Big(\frac{\partial F}{\partial\kappa}\boldsymbol{u}+\frac{\partial F}{\partial\theta'}\boldsymbol{h}_1+B\boldsymbol{h}_2-(B\boldsymbol{h}_3)'-\boldsymbol{m}_2-\frac{\partial F}{\partial\theta'}(\boldsymbol{h}_2\cdot\boldsymbol{d}')\boldsymbol{d}''\Big)\cdot\delta\boldsymbol{d}'\right]\!\!\right]\\
&\quad+\left[\!\!\left[\Big(\frac{\partial F}{\partial\theta'}\boldsymbol{h}_2+B\boldsymbol{h}_3\Big)\cdot(\boldsymbol{I}-\boldsymbol{d}'\otimes\boldsymbol{d}')\delta\boldsymbol{d}''\right]\!\!\right]+\left[\!\!\left[\frac{\partial F}{\partial\theta'}\boldsymbol{h}_3\cdot(\boldsymbol{I}-\boldsymbol{d}'\otimes\boldsymbol{d}')\delta\boldsymbol{d}'''\right]\!\!\right]\\
&=\left[\!\!\left[\Big(\frac{\partial F}{\partial\kappa}\boldsymbol{u}+\frac{\partial F}{\partial\theta'}\boldsymbol{h}_1+B\boldsymbol{h}_2-(B\boldsymbol{h}_3)'-\boldsymbol{m}_2-\frac{\partial F}{\partial\theta'}(\boldsymbol{h}_2\cdot\boldsymbol{d}')\boldsymbol{d}''\Big)\cdot\boldsymbol{g}\right]\!\!\right]\boldsymbol{g}\cdot\delta\boldsymbol{d}'\\
&\quad+\left[\!\!\left[\Big(\frac{\partial F}{\partial\kappa}\boldsymbol{u}+\frac{\partial F}{\partial\theta'}\boldsymbol{h}_1+B\boldsymbol{h}_2-(B\boldsymbol{h}_3)'-\boldsymbol{m}_2-\frac{\partial F}{\partial\theta'}(\boldsymbol{h}_2\cdot\boldsymbol{d}')\boldsymbol{d}''\Big)\cdot\boldsymbol{n}\right]\!\!\right]\boldsymbol{n}\cdot\delta\boldsymbol{d}'\\
&\qquad+\left[\!\!\left[\Big(\frac{\partial F}{\partial\theta'}\boldsymbol{h}_2+B\boldsymbol{h}_3\Big)\cdot(\boldsymbol{I}-\boldsymbol{d}'\otimes\boldsymbol{d}')\delta\boldsymbol{d}''\right]\!\!\right]+\left[\!\!\left[\frac{\partial F}{\partial\theta'}\boldsymbol{h}_3\cdot(\boldsymbol{I}-\boldsymbol{d}'\otimes\boldsymbol{d}')\delta\boldsymbol{d}'''\right]\!\!\right].
\end{aligned} \tag{B.3}$$

Since $\boldsymbol{g}\cdot\delta\boldsymbol{d}'$ and $\boldsymbol{n}\cdot\delta\boldsymbol{d}'$ can be varied arbitrarily, we obtain two jump conditions from (B.3):

$$\left.\begin{aligned}
&\left[\!\!\left[\Big(\frac{\partial F}{\partial\kappa}\boldsymbol{u}+\frac{\partial F}{\partial\theta'}\boldsymbol{h}_1+B\boldsymbol{h}_2-(B\boldsymbol{h}_3)'-\boldsymbol{m}_2-\frac{\partial F}{\partial\theta'}(\boldsymbol{h}_2\cdot\boldsymbol{d}')\boldsymbol{d}''\Big)\cdot\boldsymbol{g}\right]\!\!\right]=0,\\
&\left[\!\!\left[\Big(\frac{\partial F}{\partial\kappa}\boldsymbol{u}+\frac{\partial F}{\partial\theta'}\boldsymbol{h}_1+B\boldsymbol{h}_2-(B\boldsymbol{h}_3)'-\boldsymbol{m}_2-\frac{\partial F}{\partial\theta'}(\boldsymbol{h}_2\cdot\boldsymbol{d}')\boldsymbol{d}''\Big)\cdot\boldsymbol{n}\right]\!\!\right]=0.
\end{aligned}\right\} \tag{B.4}$$

Using the definitions (8.18), $(8.22)_2$, and $(8.22)_{1\text{–}4}$ of $F$, $\boldsymbol{m}_2$, $B$, $\boldsymbol{h}_1$, $\boldsymbol{h}_2$, and $\boldsymbol{h}_3$ in (B.4), we obtain the jump conditions (8.28).

The jump conditions (8.29) and (8.30) can be obtained by applying an argument similar to that yielding (B.4) to the remaining consequence,

$$\left[\!\!\left[\Big(\frac{\partial F}{\partial\theta'}\boldsymbol{h}_2+B\boldsymbol{h}_3\Big)\cdot(\boldsymbol{I}-\boldsymbol{d}'\otimes\boldsymbol{d}')\delta\boldsymbol{d}''\right]\!\!\right]+\left[\!\!\left[\frac{\partial F}{\partial\theta'}\boldsymbol{h}_3\cdot(\boldsymbol{I}-\boldsymbol{d}'\otimes\boldsymbol{d}')\delta\boldsymbol{d}'''\right]\!\!\right]=0, \tag{B.5}$$

of (B.3).

## References


Arroyo, J.J., Garay, Ó.J., Pámpano, Á., 2020. Boundary value problem for Euler–Bernoulli planar elastica. A solution construction procedure. J. Elasticity 139, 359–388.

Balaban, M.M., Green, A.E., Naghdi, P.M., 1967. Simple force multipoles in the theory of deformable surfaces. J. Math. Phys. 8, 1026–1036.

Chen, Y.-C., Fosdick, R., Fried, E., 2015. Representation for a smooth isometric mapping from a connected planar domain to a surface. J. Elasticity 119, 335–350.

Chen, Y.-C., Fosdick, R., Fried, E., 2018a. Isometric deformations of unstretchable material surfaces, a spatial variational treatment. J. Mech. Phys. Solids 116, 290–322.

Chen, Y.-C., Fosdick, R., Fried, E., 2018b. Issues concerning isometric deformations of planar regions to curved surfaces. J. Elasticity 132, 1–42.

Chen, Y.-C., Fried, E., 2016. Möbius bands, unstretchable material sheets, and developable surfaces. Proc. R. Soc. Lond. Ser. A Math. Phys. Eng. Sci. 472, 20150760-1–15.

Cohen, H., DeSilva, C.N., 1966. Nonlinear theory of elastic surfaces. J. Math. Phys. 7, 246–253.

Cohen, H., DeSilva, C.N., 1968. On a nonlinear theory of elastic shells. J. Méc. 7, 459–464.

Cosserat, E., Cosserat, F., 1909. Théorie des corps déformables. Hermann, Paris.

Crochet, M.J., 1971. Finite deformations of inextensible Cosserat surfaces. Int. J. Solids Struct. 7, 383–397.

Dias, M., Audoly, B., 2014. Wunderlich, meet Kirchhoff: A general and unified description of elastic ribbons and thin rods. J. Elasticity 119, 49–66.

Ericksen, J.L., Truesdell, C., 1958. Exact theory of stress and strain in rods and shells. Arch. Ration. Mech. Anal. 1, 295–323.

Euler, L., 1744. De curvis elasticis. In: Methodus inveniendi lineas curvas maximi minimive proprietate gaudentes, sive solutio problematis isoperimetrici latissimo sensu accepti. In: Chapter Additamentum I Ser. 1, vol. 24, Apud Marcum-Michaelem Bousquet & Socios, Geneva.

Green, A.E., Naghdi, P.M., Wainwright, W.L., 1965. A general theory of a cosserat surface. Arch. Ration. Mech. Anal. 20, 287–308.

Hinz, D.F., Fried, E., 2014. Translation of Michael Sadowsky's paper "An elementary proof for the existence of a developable Möbius band and the attribution of the geometric problem to a variational problem". J. Elasticity 119, 3–6.

Kirby, N.O., Fried, E., 2014. $\Gamma$-limit of a model for the elastic energy of an inextensible ribbon. J. Elasticity 119, 35–48.

Kreyszig, E., Radó, T., 1958. On rigidities of developable surfaces. J. Math. Mech. 7, 419–432.

Naghdi, P.M., 1972. The theory of shells and plates. In: Handbuch der Physik, Vol. VI a/2. Springer, Berlin.

Oldfather, W.A., Ellis, C.A., Brown, D.M., 1933. Leonhard Euler's elastic curves. Isis 20, 72–160.

O'Reilly, O.M., 2020. Intermediate Dynamics for Engineers: Newton–Euler and Lagrangian Mechanics, second ed. Cambridge University Press, Cambridge.

Sadowsky, M., 1930. Ein elementarer Beweis für die Existenz eines abwickelbaren Möbiusschen Bandes und die Zurückführung des geometrischen Problems auf ein Variationsproblem. Sitz. Preussischen Akad. Wiss. Phys.-Math. Kl. 22, 412–415.

Seguin, B., Chen, Y.-C., Fried, E., 2020. Closed unstretchable knotless ribbons and the Wunderlich functional. J. Nonlinear Sci. 30, 2577–2611.

Starostin, E.L., van der Heijden, G.H.M., 2007. The shape of a Möbius strip. Nature Mater. 6, 563–567.

Starostin, E.L., van der Heijden, G.H.M., 2014. Equilibrium shapes with stress localisation for inextensible elastic Möbius and other strips. J. Elasticity 119, 67–112.
Steigmann, D.J., 1999. On the relationship between the cosserat and Kirchhoff–Love theories of elastic shells. Math. Mech. Solids 4, 275–288.
Todres, R., 2014. Translation of W. Wunderlich's "On a developable Möbius band". J. Elasticity 119, 23–34.
Wunderlich, W., 1962. Über ein abwickelbares Möbiusband. Monatsh. Math. 66, 276–289.
Zeigler, H., 1977. Principles of Structural Stability. Springer, Basel.